Stony Brook University

On the Dynamics of Non-Linear Systems and Actuation Devices

A Dissertation Presented

by

Dake Feng

to

The Graduate School

in Partial Fulfillment of the Requirements

for the Degree of

Doctor of Philosophy

in

Mechanical Engineering

Stony Brook University

December 2014

Stony Brook University

The Graduate School

Dake Feng

We, the dissertation committee for the above candidate for the Doctor of Philosophy degree, hereby recommend acceptance of this dissertation.

Jahangir Rastegar – Dissertation Advisor
Associate Professor, Department of Mechanical Engineering

Jeffrey Ge – Chairperson of Defense
Professor, Department of Mechanical Engineering

Anurag Purwar
Associate Professor, Department of Mechanical Engineering

Harbans Dhadwal
Associate Professor
Department of Electrical Engineering

This dissertation is accepted by the Graduate School.

Charles Taber
Dean of the Graduate School

Abstract of the Dissertation

On the Dynamics of Non-Linear Systems and Actuation Devices

by

Dake Feng

Doctor of Philosophy

in

Mechanical Engineering

Stony Brook University

2014

The research results being presented in this thesis is divided into two areas. The first area is related to the development of a systematic method for model parameter identification of a large class of fully and not fully controlled nonlinear dynamics systems such as robot manipulators. The developed method is based on Trajectory Pattern Method (TPM). The developed method uses trajectory patterns with feed-forward controls to identify the system model parameters. The developed method ensures full system stability; does not require close initial estimated values for the system parameters to be identified; and provides a systematic method of

emphasizing on estimation of the parameters associated with lower order terms of the system dynamics and gradually upgrading the accuracy with which the model parameters, particularly those associated with the higher order terms of the system dynamics are estimated.

The second area of research that is being presented is related to dynamic response characteristics of electrically powered actuation systems in general and in non-linear dynamics systems in particular. Here, the term actuation systems refers to the actuator elements as well as their driving power electronics and its other related components. The study shows that the actuation forces/torques provided by such actuation systems can be divided into two basic groups. The first group corresponds to the components of the actuator force/torque that is "actuator motion independent". The dynamic response of this group is relatively high and limited only by the dynamic response limitations - for the case of electrically driven actuation systems - of the driving power amplifiers, electronics, computational and signal processing devices and components. The second group corresponds to those components of the actuator forces/torques that is "actuator motion dependent". The dynamic response of this group is relatively low and dependent on the actuator effective inertial load and actuation speed. In all mechanical systems that are properly designed, the dynamic response of the first group is significantly higher than those of the second group.

By separating the required actuating forces/torques into the above two groups, the dynamic response of such nonlinear dynamics systems may be determined for a given synthesized trajectory. The information can also be used to significantly increase the performance of control systems of such mechanical systems.

Contents

List of Figures

List of Tables

Acknowledgements

I would never have been able to finish my dissertation without the guidance of my committee members, help from friends, and support from my family, parents, wife and daughters.

I would like to express my deepest gratitude to my advisor, Dr. Jahangir Rastegar, for his excellent guidance, caring, patience, and providing me with an excellent atmosphere for doing research.

I would also like to thank my parents. They were always supporting me and encouraging me with their best wishes.

I want to express my deepest appreciation to my lovely sweet daughters, Harmony, Danica and Melody, for their great patience and understandings. Finally, I would like to thank my wife, Hanchao. She was always there cheering me up and stood by me through the good times and bad.

Chapter 1

Introduction

The dynamics of machines such as robot manipulators and those constructed with linkage mechanisms, particularly those operating at relatively high speeds, is highly nonlinear. The dynamics of such mechanical systems constructed with relatively rigid links, which are considered as fully controlled, or flexible links, which are considered as not fully controlled, can be modeled as ordinary differential equations that are linear-in-parameters. Such models accurately represent a large class of mechanical systems and usually employ appropriate actuation and controls to form nonlinear dynamics systems.

Identification of the model parameters of such systems such as their kinematics and dynamics (inertia) parameters is important for accurate prediction of the dynamic behavior of the system, and for the system design, path and trajectory planning and synthesis, and their control. In particular, accurate identification of model parameters is essential for the control of high-speed and ultra-precision machines, especially when model-based methods are required to achieve the desired system performance.

A review of the published literature indicates that a systematic method for parameter identification of highly nonlinear and linear-in-parameter mechanical systems such as robot manipulators or other similar computer controlled machines, particularly if they are desired to operate at high-speeds with very high precision has not yet been developed.

In this thesis, a new systematic method for model parameter identification of highly nonlinear and linear-in-parameter mechanical systems, fully controlled and non-fully controlled, are presented and the mathematical proof of its stability and convergence is provided. The method is based on the Trajectory Pattern Method. In this method, for a pattern of motion the inverse dynamics model of the system is derived in algebraic form in terms of the trajectory pattern parameters. The system dynamics model parameters are then identified using a systematic algorithm which ensures system stability as well as accurate estimation of the model parameters associated with lower as well as higher order dynamic terms. The method is shown to be fast converging and does not require initial close estimation of system parameters in order to ensure convergence.

On the other hand, the dynamics of actuation devices of different types have been extensively studied. However, a review of published literature indicates that dynamic response issues have not been fully explained for nonlinear dynamics systems, including mechanical systems such as robot manipulators. In most current approaches to path and trajectory synthesis and control of mechanical systems, methods used for linear dynamics systems are generally employed while treating the effects of nonlinearity as input disturbances. For highly nonlinear dynamics systems, this usually means that the system opera-

tion must be relatively slow to ensure stability and effectiveness of the control system in providing operational precision. Model based feed-forward control algorithms are also used to minimize the effects of the nonlinear components of the system dynamics and to achieve better system performance in terms of operating speed and precision.

The lack of full understanding of the dynamic response characteristics and limitations of the actuation systems of mechanical systems with highly nonlinear dynamics, however, significantly reduces the effectiveness of their control system.

This thesis presents study clearly showing that the actuation forces/torques provided by actuation devices driving mechanical systems can be divided into two basic groups. The first group corresponds to those components of each actuator force/torque that are "actuator motion independent". The dynamic response of this group is shown to be relatively high and limited only by the dynamic response limitations - for the case of electrically driven actuation systems - of the driving power amplifiers, electronics, computational and signal processing devices and components. The second group corresponds to those components of the actuator forces/torques that are "actuator motion dependent". The dynamic response of the latter group is shown to be relatively low and dependent on the actuator effective inertial load and actuation speed. In all mechanical systems that are properly designed, the dynamic response of the first group is significantly higher than those of the second group. By separating the required actuating forces/torques into the above two groups, the characteristics of the dynamic response of such nonlinear dynamics systems may be determined for a prescribed trajectory. The information can also

be used to significantly increase the performance of control systems of such mechanical systems by properly synthesized trajectories and control. When a feed-forward control signal is used, the performance of the system is shown to be significantly improved by generating each one of the aforementioned group of components separately considering the dynamic response of the actuation system to each one of the groups of components.

This thesis consists of six chapters. The material presented in each of the four chapters following the introduction, Chapter 1, is in most part self contained. In most chapters, a literature review of the related topics precedes the main text, and is followed by a discussion and conclusion section. The illustrations and tables are placed at the end of the corresponding chapter. The references are listed in alphabetical order at the end of the thesis. The following is a brief description of the material presented in each chapter of this thesis.

In Chapter 2, the lowest harmonic trajectory pattern that can be synthesized for point-to-point motions with zero end point velocity, acceleration and jerk of fully controlled nonlinear dynamics system such as robot manipulators with rigid links are derived and the proof of their existence are provided. It is also shown that for such fully controlled dynamic systems, such trajectory patterns would require actuating forces/torques with the minimum possible number of harmonic content.

In Chapter 3, a systematic method for parameter identification of highly nonlinear, linear-in-parameter and fully controlled mechanical systems such as robot manipulators or other similar computer controlled machines, particularly if they are desired to operate at high-speeds with very high precision is

presented. Such a method guarantees that the system stays stable at all times during the identification process and that it can accurately identify parameters that contribute to the higher order dynamics terms, particularly those that become significant at higher operating speeds.

In Chapter 4, a systematic method for parameter identification of highly nonlinear, non-fully controlled and linear-in-parameter mechanical systems such as robot manipulators or other similar computer controlled machines constructed with flexible structure, particularly if they are desired to operate at high-speeds with very high precision is presented. Such a method is guarantees that the system stays stable at all times during the identification process and that it can accurately identify parameters that contribute to the higher order dynamics terms, particularly those that become significant at higher operating speeds.

In Chapter 5, an experiment is designed to prove the parameter identification method. A highly nonlinear two degrees of freedom manipulator is built. The controller adopts Digital Signal Processor as realtime feedback/feedforward system and the velocity, position decoder is based on field-programmable gate array. The experiment follows the proposed procedure in chapter 3, and the result shows convergence of model parameter identification.

In Chapter 6, it presents a totally new approach at studying the dynamic response requirements of mechanical systems with open-loop kinematic chain and nonlinear dynamics such as robot manipulators. It is shown that the dynamic response requirements of the system actuators can be associated with two different groups of components. The first group is shown to correspond to the components of each actuator force/torque that is "*actuator motion inde-*

pendent". The dynamic response of this group of components of the actuating forces/torques is shown to be limited only by the dynamic response limitations - for the case of electrically driven actuation systems - of the driving power amplifiers, electronics, computational and signal processing devices and components. The second group corresponds to the components of each actuator force/torque that is "*actuator motion dependent*". The dynamic response of this group of components of the actuator forces/torques is limited mainly by the effective inertia that is experienced by the actuator and its operating speed. Due to the nature of the currently available electrical, hydraulic and other actuation systems, the dynamic response of actuation systems is shown to be generally high to the former group of components and significantly lower to the latter group of components.

Chapter 2

On The Minimum Harmonic Trajectory Pattern For Point-To-Point Motion

2.1 Introduction

For trajectory synthesis of robot manipulators and computer controlled machines, polynomial and spline curves have been widely used [1, 2]. Johnson, et al. in [3] developed a trajectory optimization technique for synthesizing dynamically feasible trajectories for mechanical system that approximate a desired trajectory. Korayem, et al. reported another trajectory synthesis method for optimizing point-to-point motions using the Pontryagin's minimum principle and solving a two-point boundary value problem [4]. When expressed in Fourier series, all such trajectories contain a considerable number of high harmonic components. In systems such as robot manipulators, the nonlinear-

ity of their kinematics and dynamics will also generate a significant number of harmonics of the harmonics present in the trajectory, thereby requiring the actuating torques/forces to contain very harmonic content, usually way above their dynamic response capabilities, particularly for relatively high-speed motions. As a result, the system becomes incapable of tracking the synthesized trajectory with precision. In addition, the harmonics present in the actuating torques/forces may have frequencies that are close to the natural modes of vibration of the system and therefore cause vibration and control problems as the manipulator attempts to follow the synthesized trajectory.

The concept of Trajectory Patterns was introduced for synthesis of trajectories with low harmonic content [5, 37, 39] for high-speed and precision motions with minimal excitation of the natural modes of vibration of a system. Trajectory patterns are classes of joint trajectories formed by an appropriate number of basic time functions with a number of trajectory parameters [8]. This method has been shown to be most appropriate for low harmonic motion synthesis, with the consideration of limitations of the actuator dynamic response. Therefore such trajectories can be utilized to synthesize motions with minimal actuator high harmonic content [9].

In this chapter, the lowest harmonic trajectory pattern that can be synthesized for point-to-point motions with zero end point velocity, acceleration and jerk of fully controlled nonlinear dynamics system such as robot manipulators with rigid links are derived and the proof of their existence are provided. It is also shown that for such fully controlled dynamic systems, such trajectory patterns would require actuating forces/torques with the minimum possible number of harmonic content.

2.2 The Lowest Harmonic Trajectory Pattern For Point-To-Point Motions

The simplest harmonic trajectory pattern is the one formed by a fundamental sinusoidal time function and $(n-1)$ number of its harmonics as described by

$$x(t) = \sum_{i=0}^{n} [a_i \cos i\omega t + b_i \sin i\omega t] \tag{2.1}$$

Where x is the synthesized motion, t is time, a_i and b_i are the trajectory parameters corresponding to the ith trajectory harmonic, and ω is its fundamental frequency.

Let the point-to-point motion to be synthesized start at the point x_0 at time $t = 0$ and end at x_1 at time $t = t_1$. For a point-to-point motion with zero end point acceleration and jerk, the trajectory must satisfy the following eight end conditions

$$x(0) = \sum_{i=0}^{n} a_i = x_0 \tag{2.2}$$

$$x(t_1) = \sum_{i=0}^{n} [a_i \cos i\omega t_1 + b_i \sin i\omega t_1] = x_1 \tag{2.3}$$

$$\dot{x}(0) = \sum_{i=1}^{n} i\omega b_i = 0 \tag{2.4}$$

$$\dot{x}(t_1) = \sum_{i=1}^{n} i\omega [-a_i \sin i\omega t_1 + b_i \cos i\omega t_1] = 0 \tag{2.5}$$

$$\ddot{x}(0) = \sum_{i=1}^{n} -i^2\omega^2 a_i = 0 \tag{2.6}$$

$$\ddot{x}(t_1) = \sum_{i=1}^{n} i^2\omega^2[-a_i \cos i\omega t_1 - b_i \sin i\omega t_1] = 0 \tag{2.7}$$

$$\dddot{x}(0) = \sum_{i=1}^{n} -i^3\omega^3 b_i = 0 \tag{2.8}$$

$$\dddot{x}(t_1) = \sum_{i=1}^{n} i^3\omega^3[a_i \sin i\omega t_1 - b_i \cos i\omega t_1] = 0 \tag{2.9}$$

To satisfy the above eight end conditions, the trajectory pattern of Eqn. (2.1) must in general have a minimum of four harmonics, i.e., for a given fundamental frequency ω, the trajectory pattern must contain at least three harmonics of the fundamental frequency, i.e., n must be at least equal to 4.

It is, however, shown below that special type of trajectory patterns do exist in which such point-to-point motions with zero end point accelerations and jerks can be synthesized with a fundamental frequency and its second harmonic. It is also shown that this trajectory pattern constitutes the lowest possible harmonic point-to-point trajectory that can be synthesized with zero end point accelerations and jerks.

Firstly, from Eqns. (2.4) and (2.8), it is readily observed that by setting $b_i = 0$, these two end conditions would always be satisfied and the total number of end conditions to be satisfied drops to 6 from 8.

Secondly, by examining the end conditions of Eqns. (2.5) and (2.9), it is readily observed that by setting the time t_1 to the half of fundamental harmonic period, i.e., if $t_1 = \frac{\pi}{\omega}$, the latter two end conditions would always be satisfied,

thereby reducing the number of end conditions to be satisfied for each motion to be synthesized to 4 as

$$x(0) = \sum_{i=0}^{n} a_i = x_0 \tag{2.10}$$

$$x(\frac{\pi}{\omega}) = \sum_{i=0}^{n} a_i(-1)^i = x_1 \tag{2.11}$$

$$\ddot{x}(0) = \sum_{i=1}^{n} -i^2\omega^2 a_i = 0 \tag{2.12}$$

$$\ddot{x}(\frac{\pi}{\omega}) = \sum_{i=1}^{n} -i^2\omega^2 a_i(-1)^i = 0 \tag{2.13}$$

Thirdly, by adding and subtracting Eqns.(2.12) and (2.13), the following relationships between the coefficients a_i are derived (here, $[\frac{n}{2}]$ is defined as the integer of $\frac{n}{2}$):

$$\sum_{k=0}^{[\frac{n}{2}]} a_{2k+1}(2k+1)^2\omega^2 = 0 \tag{2.14}$$

$$\sum_{k=1}^{[\frac{n}{2}]} a_{2k}(2k)^2\omega^2 = 0 \tag{2.15}$$

Eqns.(2.14) and (2.15) indicate that certain relationship must exist between the amplitudes of the odd and even harmonics of the trajectory pattern. Now by setting the amplitudes of the even harmonics to zero, i.e., by setting $a_{2k} = 0$, $k = 1, 2, ...$, the Eqn.(2.15) is then satisfied for all trajectories and the number of end condition relationships to be satisfied is reduced to 3. The first two of the relationships correspond to the end positions, Eqns.(2.10) and (2.11), and

one relates the amplitudes of the odd harmonic components, Eqn.(2.14).

As a result, the lowest harmonic trajectory that can satisfy the aforementioned end condition related relationships, Eqns.(2.10), (2.11) and Eqn.(2.14), becomes

$$x(t) = a_0 + a_1 \cos(\omega t) + a_3 \cos(3\omega t) \tag{2.16}$$

From which we can solve for the three trajectory pattern parameters a_0, a_1 and a_3 as

$$a_0 = \frac{x_0 + x_1}{2} \tag{2.17}$$

$$a_1 = \frac{9(x_0 - x_1)}{16} \tag{2.18}$$

$$a_2 = \frac{-x_0 + x_1}{16} \tag{2.19}$$

By substituting Eqns.(2.17), (2.18) and (2.19) into Eqn.(2.16), the synthesized lowest harmonic trajectory pattern is obtained as

$$x(t) = \frac{x_0 + x_1}{2} + \frac{9(x_0 - x_1)}{16} \left[\cos(\omega t) - \frac{1}{9} \cos(3\omega t) \right] \tag{2.20}$$

Taking advantage of the symmetry of the trajectory pattern of Eqn.(2.20), the trajectory pattern can be expressed as

$$x(t) = \lambda(\cos \omega t - \frac{1}{9} \cos 3\omega t) \tag{2.21}$$

where λ is a parameter indicating the starting position of the synthesized point-to-point motion as $x(0) = \frac{8}{9}\lambda$ and the end position as $x(\frac{\pi}{\omega}) = -\frac{8}{9}\lambda$. ,

The unique trajectory pattern of Eqn.(2.20) or its equivalent (2.21) is thereby shown to represent the lowest possible harmonic point-to-point motion with zero end accelerations and jerk.

2.3 Actuation Forces/Torques Pattern for Lowest Harmonic Point-to-Point Trajectory Patterns

For fully controlled dynamic systems such as robot manipulators and computer controlled machines with rigid links, the differential equations of motion may be readily described in the following polynomial form (see [5, 8, 37, 39]]

$$m\ddot{x} + \sum_{i=0,j=0}^{p,q} k_{ij}\dot{x}^i x^j = u \tag{2.22}$$

where p, q are non-negative integers indicating the highest order term of $\dot{x}$ and x with significant amplitude, u is the system input (actuating force or torque), x is the system output (displacement or rotation), and m and $k_{i,j}$ are the system kinematics and dynamics parameters.

2.3.1 Harmonic Components of the Actuating Forces/Torques

For a dynamics system represented by the non-linear differential equation Eqn. (2.22) following the lowest harmonic point-to-point trajectory of Eqn. (2.21),

the required actuating force/torque is readily shown to become

$$\begin{aligned} u(t) &= m\ddot{x}(t) + \sum_{i=0,j=0}^{p,q} k_{ij}\dot{x}(t)^i x(t)^j = m\lambda\omega^2(-\cos\omega t + \cos 3\omega t) \\ &+ \sum_{i=0,j=0}^{p,q} k_{ij}\omega^i\lambda^{i+j}(-\sin\omega t + \frac{1}{3}\sin 3\omega t)^i(\cos\omega t - \frac{1}{9}\cos 3\omega t)^j \end{aligned} \tag{2.23}$$

Expanding the term $(-\sin\omega t + \frac{1}{3}\sin 3\omega t)^i$, when i is an even integer, then

$$(-\sin\omega t + \frac{1}{3}\sin 3\omega t)^i = \sum_{l=0}^{\frac{3i}{2}} a_l \cos(2l)\omega t \tag{2.24}$$

And when i is an odd integer, then

$$(-\sin\omega t + \frac{1}{3}\sin 3\omega t)^i = \sum_{l=0}^{\frac{3i-1}{2}} a'_l \sin(2l+1)\omega t \tag{2.25}$$

where a_l, a'_l are the amplitude coefficients for the corresponding harmonic functions.

And expanding the term $(\cos\omega t - \frac{1}{9}\cos 3\omega t)^j$, when j is an even integer, then

$$(\cos\omega t - \frac{1}{9}\cos 3\omega t)^j = \sum_{l=0}^{\frac{3j}{2}} b_l \cos(2l)\omega t \tag{2.26}$$

And when j is an odd integer,

$$(\cos\omega t - \frac{1}{9}\cos 3\omega t)^j = \sum_{l=0}^{\frac{3j-1}{2}} b'_l \cos(2l+1)\omega t \tag{2.27}$$

where b_l, b'_l are the amplitude coefficients for the corresponding harmonic functions.

Therefore the highest harmonic present in the term

$$(-\sin\omega t + \frac{1}{3}\sin 3\omega t)^i(\cos\omega t - \frac{1}{9}\cos 3\omega t)^j$$

of the Eqn. (req-actuator-force) has a frequency of $3(i+j)\omega$. Thus, the highest frequency component that the actuating force/torque $u(t)$ has to provide has a frequency of

$$\omega_{max} = 3(p+q)\omega \tag{2.28}$$

where $(p+q)$ is defined by the system dynamics, indicating the highest significant order of the dynamics of the system, and 3ω is the highest harmonic component in the trajectory pattern to be followed.

It can therefore be concluded that the trajectory pattern with the lowest number of harmonics of Eqn. (2.21) for point-to-point motions with zero end point accelerations and jerks would also demand actuating forces/torques with the lowest number of harmonics. It is obvious that trajectories with non-zero end point accelerations and jerks would demand significantly higher actuating force/torque harmonics due to the required actuating force/torque discontinuities.

2.4 Conclusions

Trajectory pattern with lowest number of harmonics for point-to-point motions of fully controlled dynamic systems with zero end point accelerations and jerks

is shown to be unique and is presented together with its proof of existence and uniqueness. For such fully controlled dynamics systems such as robot manipulators with rigid links or other similar computer controlled machines, it is also shown that the actuating forces/torques required for the system to track such trajectory patterns also generally contain the lowest possible harmonic content.

Trajectory patterns with low harmonic content and low harmonic content of the required actuating forces/torques to track the synthesized trajectories are important, particularly for higher operating speeds, due to vibration and control problems and since the frequency of the highest harmonic present in the actuating force/torque may exceed the dynamic response limit of the system actuation devices.

Chapter 3

Model Parameter Identification for Fully Controlled Nonlinear Dynamic System

3.1 Introduction

The dynamics of machines such as robot manipulators and those constructed with linkage mechanisms, particularly those operating at relatively high speeds, is highly nonlinear. The dynamics of such mechanical systems constructed with relatively rigid links can be modeled as ordinary differential equations that are linear-in-parameters. Such models accurately represent a large class of mechanical systems and usually employ appropriate actuation and controls to form fully controlled nonlinear dynamics systems.

Identification of the model parameters of such systems such as their kinematics and dynamics (inertia) parameters is important for accurate prediction

of the dynamic behavior of the system, and for the system design, path and trajectory planning and synthesis, and their control (e.g., see [13]). In particular, accurate identification of model parameters is essential for the control of high-speed and ultra-precision machines, especially when model-based methods are required to achieve the desired system performance.

A number of investigators have developed procedures for the identification and calibration of the kinematics parameters of various mechanical systems, e.g., Ibarra and Perreira [14], Kazerounian and Qian [15], Goswami and Bosnik [16], Kaizerman, et al. [17] and Zak, et al. [18]. Others have contributed to the development of dynamics parameter identification techniques. For example, Guo and Angeles [19] developed a method for linearized systems for on-line recursive least square parameter estimation for feedback gains. Kawasaki and Nishimura [20] developed a method called "instrument variable method" (IVM) which yields more accurate estimation than least square methods (LSM). Based on a statistical framework, Swevers, et al. [21] formulated a maximum-likelihood estimation method for the dynamics parameters of robot models. Lin [22] developed a method which does not require symbolic dynamics equations to identify the inertia parameters of a manipulator. In another study, Lin [23] showed an approach to identify the parameters of a manipulator based on the least square method. Dolanc and Strmcnik [24] used a piecewise-linear Hammerstein excitation signal for parameter estimation of nonlinear systems. Kenne, et al. [25] employed radial basis function networks for time varying parameter estimation of nonlinear systems. Spottswood and Allemang [26] proposed a frequency domain approach called "Modified Feedback of the Output Method" for parameter identification of reduced order

nonlinear models.

Other related research has been in the area of the development of methods to identify the structure of appropriate models for nonlinear dynamics systems, including the present linear-in-parameters systems. For example, Li, et al. [27] developed a two-stage algorithm for identification of the structure of nonlinear dynamics systems in which an initial model is built from a large pool of basis functions or model terms and the significance of each term is evaluated. Gray, et al. [28] used a similar method together with Genetic Programming for nonlinear model structure identification. This method is an optimization method which automatically selects model structure elements from a database. Abdelazim and Malik [29] used a fuzzy logic grey box modeling technique for identification of the structure of nonlinear dynamics systems. Other published literature in the area of parameter identification for nonlinear linear-in-the-parameters dynamics system includes those Chen, et al. [30], Poroddi and Spinelli [31], and Zhu and Billings [32].

A review of the published literature indicates that a systematic method for parameter identification of highly nonlinear and linear-in-parameter mechanical systems such as robot manipulators or other similar computer controlled machines, particularly if they are desired to operate at high-speeds with very high precision has not yet been developed. Such a method is required to guarantee that the system stays stable at all times during the identification process and that it can accurately identify parameters that contribute to the higher order dynamics terms, particularly those that become significant at higher operating speeds.

In this chapter, the development of such a method is presented. The

method is based on the Trajectory Pattern Method [13, 33–40]. The method is robust and is applicable to highly nonlinear dynamics systems and does not require accurate initial estimation of the system parameters. Presented in this chapter is a comprehensive description and mathematical proof of the developed method, a preliminary study of which was presented in [**?**]. Examples are also provided of its implementation on highly nonlinear dynamics systems.

3.2 Model Parameter Identification Based On Trajectory Patterns

The method being described in this chapter is for the identification of parameters of a large class of nonlinear dynamics systems that are fully controlled and are linear-in-parameter. Such systems include various machines such as robot manipulators and other similar computer controlled machinery that can be considered to be constructed with rigid links. A dynamics model that adequately describes the dynamic behavior of the system is considered to be provided. The model parameters are, however, not accurately known and are needed to be identified. The model parameters are considered to be constant, but the present method can be used for on-line updating of time varying parameters as long as the changes are relatively slow.

3.2.1 Trajectory Pattern Method

The present model parameter identification method is based on the Trajectory Pattern Method (TPM) [13, 33–40]. In TPM, a trajectory pattern is

a collection of appropriate basic time functions with certain number of fixed (trajectory) parameters with which the desired trajectories are synthesized. During trajectory synthesis, the trajectory parameters are determined such that the desired motion is realized. The synthesized motions may be point to point, tracking, or regulatory (e.g., for vibration suppression) in nature. The inverse dynamics model of a system is then derived in parametric form for the selected trajectory (motion) patterns. The motions may be synthesized using some optimality criterion such as minimum cycle time. The trajectory patterns that appear to be most advantageous are those constructed using a number of basic sinusoidal time functions and their harmonics. In which case, the resulting actuation forces (control signals) become in terms the basic sinusoidal time functions and a number of their harmonics. The number of harmonics that appear in the actuation torques is dependent on the degree of nonlinearity of the dynamics of the system. This permits the selection (synthesis) of those motions that do not contain the natural modes of oscillation of the system. During the motion, the natural modes of vibration of the system are therefore not excited. In addition, by limiting the frequency of the highest harmonic of the actuation signals during the motion synthesis, one can ensure that the system actuators can meet the dynamic response requirements of the system.

For a selected trajectory pattern, the structure of the inverse dynamic model is fixed. This makes it possible to derive analytical relationships between the parameters of the system (model), the trajectory parameters, and the control signal parameters. The formulation involves pure algebraic manipulations. Obviously, the degree of complexity of the derivations involved

and the amount of algebraic manipulations that need to be performed are dependent on the complexity of the dynamics of the system and the selected trajectory pattern. In the work being presented, this characteristic of the TPM is utilized to develop a systematic method and related algorithms to identify the parameters of the model of such nonlinear dynamics systems.

3.2.2 Model Parameter Identification Method

In this section, the developed systematic method for identification of the parameters of the class of fully controlled nonlinear dynamics systems such as serial robot manipulators with relatively rigid links is described and the mathematical proof of its convergence and stability during the identification process is provided for a system with one degrees-of-freedom. The method can be seen to be readily extendable to multi-degrees-of-freedom systems. The dynamics of such systems are described by ordinary differential equations in the form of so-called linear-in-the-parameters nonlinear systems [27].

The dynamics of the class of fully controlled and linear-in-the-parameters nonlinear dynamics systems of interest can be described in the following form

$$m\ddot{x} + D(x, \dot{x}, k_1, k_2, ..., k_n) = u \tag{3.1}$$

where x is the system output, u is the system input, m, k_1, k_2,..., k_n are the n+1 system parameters to be identified. It is readily shown that the nonlinear term D can be accurately expressed in polynomial form using Taylor series as shown in [13, 33–40] for robot manipulators with serial rigid link. The nonlinear term

D can thereby be expressed in the following form

$$D(x, \dot{x}, k_1, k_2, ..., k_n) = \sum_{j=1}^{n} k_j x^{p_j} \dot{x}^{q_j} \tag{3.2}$$

where p_j and q_j are non-negative integer exponents of x and $\dot{x}$, respectively, in the jth term of the polynomial.

Now consider the trajectory pattern

$$x_r = \lambda \left[\cos(\omega t) - \frac{1}{9} \cos(3\omega t) \right] \tag{3.3}$$

where x_r is the desired motion, ω is the fundamental frequency of the trajectory and one of the trajectory parameters and λ is the other trajectory parameter. With the motion starting at time $t = 0$ and ending at time $t = \pi/\omega$, i.e., half the period of the fundamental frequency ω, this trajectory pattern provides smooth point-to-point motions with zero initial and final velocity, acceleration and jerk. In this trajectory pattern, the time to complete the point-to-point motion is determined by the trajectory parameter (fundamental frequency) ω, and the trajectory parameter λ indicates the total distance traveled during the motion. The trajectory pattern (4.13) has low harmonic content, thereby is suitable for synthesizing point-to-point motions in nonlinear dynamics systems since it can be expected to demand lower actuating force/torque harmonics. As a result, lower dynamic response is generally required from the actuation devices as compared to arbitrarily synthesized trajectories. The fundamental frequency ω can also be selected such that the natural modes of vibration of the system are not excited in resonance during the motion.

In the present method, a feed-forward control system with a feedback loop is used to achieve full system control, as shown in Figure 3.1. The feed-forward signal f_f is calculated from the inverse dynamics model of the system, Eqn. (4.1), with the estimated system parameters m, k_1, k_2,..., k_n. The feedback gains of the linear controller are considered to be large enough to achieve accurate trajectory tracking. It is shown later in this section that with the trajectory pattern Eqn. (4.13) and by selecting appropriate values for the trajectory parameters ω and λ, i.e., for relatively slow (small trajectory parameter ω) and small point-to-point motions (small trajectory parameter λ), any nonlinear dynamics system of the form Eqn. (4.1) can be forced to accurately follow the synthesized trajectory with an appropriately designed actuation device and a linear feedback control with high enough gains.

In the present method, the feed-forward signal f_f, Figure 3.1, is calculated from the dynamics model of the system, Eqn. (4.1), with the specified trajectory pattern, such as the trajectory pattern Eqn. (4.13). Since the system parameters are not yet known, their estimated values, denoted here as m', k'_1 , k'_2 ,..., k'_n are used to calculate the feed-forward signal as

$$f_f = m'\ddot{x}_r + D(x_r, \dot{x}_r, k'_1, k'_2, ..., k'_n) \tag{3.4}$$

The control loop dynamics, Fig. 1, can be seen to be described by

$$m\ddot{x} + D(x, \dot{x}, k_1, k_2, ..., k_n) = f_f + C(e) \tag{3.5}$$

where $C(e)$ is the control signal and e is the error $e = x_a - x_r$, where x_a is the

system output. Substituting x_a with $x_r + e$ in Eqn. (4.15), we get

$$m\ddot{e} + m\ddot{x_r} + D(x_r + e, \dot{x_r} + \dot{e}, k_1, k_2, ..., k_n) = f_f + C(e) \tag{3.6}$$

However, since D in Eqn. (4.16) is a polynomial function, it can be rearranged into the following form

$$\begin{aligned} D(x_r + e, \dot{x_r} + \dot{e}, k_1, k_2, ..., k_n) = D(x_r, \dot{x_r}, k_1, k_2, ..., k_n) + \\ D(e, \dot{e}, k_1, k_2, ..., k_n) + D'(x_r, e, \dot{x_r}, \dot{e}, k_1, k_2, ..., k_n) \end{aligned} \tag{3.7}$$

where the term D' is another polynomial function whose order is one less than the term D. By substituting Eqns. (4.17) and (4.14) into Eqn. (4.16) and rearranging the resulting equation, we get

$$\begin{aligned} m\ddot{e} \quad + \quad D(e, \dot{e}, k_1, k_2, ..., k_n) + D'(x_r, e, \dot{x_r}, \dot{e}, k_1, k_2, ..., k_n) = m'\ddot{x_r} - \\ m\ddot{x_r} \quad + D(x_r, \dot{x_r}, k_1', k_2', ..., k_n') - D(x_r, \dot{x_r}, k_1, k_2, ..., k_n) + C(e) \end{aligned} \tag{3.8}$$

and since the terms D and D' are polynomial functions in which the parameters $k_i s$ and $k_i' s$ are coefficients of the polynomial terms, therefore the functions D and D' are linear with respect to the parameters $k_i s$ and $k_i' s$. The first four terms on the right hand side of Eqn. (4.18) can be simplified to

$$\begin{aligned} m'\ddot{x_r} - m\ddot{x_r} \quad + D(x_r, \dot{x_r}, k_1', k_2', ..., k_n') - D(x_r, \dot{x_r}, k_1, k_2, ..., k_n) = \\ \Delta m\ddot{x_r} + D(x_r, \dot{x_r}, \Delta k_1, \Delta k_2, ..., \Delta k_n) \end{aligned} \tag{3.9}$$

where $\Delta m = m' - m$ and $\Delta k_i = k'_i - k_i$ are errors in the estimated parameter values m and k_i, $i = 1, 2, ..., n$.

Then substituting Eqn. (4.19) into Eqn. (4.18), we get

$$m\ddot{e} + D(e, \dot{e}, k_1, k_2, ..., k_n) + D'(x_r, e, \dot{x_r}, \dot{e}, k_1, k_2, ..., k_n) = \Delta m\ddot{x_r} + D(x_r, \dot{x_r}, \Delta k_1, \Delta k_2, ..., \Delta k_n) + C(e) \tag{3.10}$$

Now consider the use of a linear controller such as a PD controller $C(e) = G_1\dot{e} + G_2 e$, where G_1 and G_2 are the proportional and derivative gains with large enough values for the selected trajectory pattern parameters. By substituting the control signal $C(e)$ into Eqn. (4.20) and expanding the terms D and D' into their polynomial forms, we get

$$m\ddot{e} + \sum_{j=1}^{n} k_j e^{p_j} \dot{e}^{q_j} + \sum_{j=1}^{n} k_j \sum_{i,l=1}^{j} c_{jil} e^i \dot{e}^{p_j - i - 1} x_r^l \dot{x}_r^{q_j - l - 1} = \Delta m\ddot{x_r} + \sum_{j=1}^{n} \Delta k_j x_r^{p_j} \dot{x}_r^{q_j} + G_1\dot{e} + G_2 e \tag{3.11}$$

where c_{jil} are the coefficients in the expanded term D'.

Rearranging Eqn. (3.11) by bringing all e and $\dot{e}$ terms to the left hand side and neglecting all their higher order terms since both e and $\dot{e}$ terms can be forced to become very small by the selection of small trajectory parameters λ and ω and large enough controller gains, we get

$$m\ddot{e} - G_1\dot{e} - G_2 e = \Delta m\ddot{x_r} + \sum_{j=1}^{n} \Delta k_j {x_r}^{p_j} {\dot{x}_r}^{q_j} \tag{3.12}$$

As expected, with the assumption of small enough trajectory parameters λ

and ω and large enough controller gains, the differential equation describing the error becomes linear. As can be observed, the requirement of "close enough" model parameter estimates in general feedforward control has been replaced by the requirement of "small enough" trajectory parameters λ and ω to ensure stability with closely approximated linear differential equation describing the system tracking error, Eqn. (4.21). This means that by using the developed trajectory pattern method, the system parameters of fully controlled nonlinear dynamics systems such as robot manipulators with rigid links can be identified without the availability of good estimated values for the system parameters as described below.

By substituting the selected trajectory pattern Eqn. (4.13) into the right hand side of Eqn. (4.21), we get

$$\begin{aligned} \Delta m\ddot{x}_r + \quad & \sum_{j=1}^{n} \Delta k_j x_r^{p_j} \dot{x}_r{}^{q_j} = [\Delta m\lambda\omega^2][-\cos(\omega t) + \cos(3\omega t)] + \\ & \sum_{j=1}^{n} \left\{ (\Delta k_j \lambda^{p_j+q_j} \omega^{q_j})[\cos(\omega t) - \frac{1}{9}\cos(3\omega t)]^{p_j} \right. \\ & \left. [-\sin(\omega t) + \frac{1}{3}\sin(3\omega t)]^{q_j} \right\} \end{aligned} \tag{3.13}$$

which can be written as

$$\Delta m\ddot{x}_r + \sum_{j=1}^{n} \Delta k_j x_r^{p_j} \dot{x}_r^{q_j} = a_0 + \sum_{i=1}^{N} [a_{ci}\cos(i\omega t) + a_{si}\sin(i\omega t)] \tag{3.14}$$

where N is the highest harmonic component present in the error as the system is forced to follow the trajectory pattern Eqn. (4.13). From Eqn. (3.13), it can be seen that N is $3(p_n + q_n)$.

Now as can be seen from Eqn. (3.13), the amplitudes a_0, a_{ci} and a_{si} of the

harmonics present in the Eqn. (4.22) can be expressed as a linear combination of the errors in the estimated values of the system parameters, i.e., Δm and Δk_j in the present system described by Eqn. (4.1). Thus, by defining constants b_{ij} as the coefficients of the expanded trigonometric polynomials in Eqn. (3.13) (the underscore $\_$ standing for either s or c), the amplitudes a_0 and $a_{\_i}$ can be expressed as

$$a_0 = b_0\lambda\omega^2\Delta m + \sum_{j=1}^{n} b_{0j}\lambda^{p_j+q_j}\omega^{q_j}\Delta k_j \tag{3.15}$$

$$a_{\_i} = b_{\_i0}\lambda\omega^2\Delta m + \sum_{j=1}^{n} b_{\_ij}\lambda^{p_j+q_j}\omega^{q_j}\Delta k_j \tag{3.16}$$

or in matrix form as

$$\begin{aligned}
[a_0] &= \mathbf{B}_0 \begin{bmatrix} \lambda\omega^2 & 0 & ... & 0 \\ 0 & \lambda^{p_1+q_1}\omega^{q_1} & ... & 0 \\ ... & ... & ... & ... \\ 0 & 0 & ... & \lambda^{p_n+q_n}\omega^{q_n} \end{bmatrix} \begin{bmatrix} \Delta m \\ \Delta k_1 \\ ... \\ \Delta k_n \end{bmatrix} \\
\begin{bmatrix} a_{ci} \\ a_{si} \end{bmatrix} &= \mathbf{B}_i \begin{bmatrix} \lambda\omega^2 & 0 & ... & 0 \\ 0 & \lambda^{p_1+q_1}\omega^{q_1} & ... & 0 \\ ... & ... & ... & ... \\ 0 & 0 & ... & \lambda^{p_n+q_n}\omega^{q_n} \end{bmatrix} \begin{bmatrix} \Delta m \\ \Delta k_1 \\ ... \\ \Delta k_n \end{bmatrix}
\end{aligned} \tag{3.17}$$

where $\mathbf{B}_0 = [b_0\, b_{01} \,...\, b_{0n}]$, $\mathbf{B}_i = \begin{bmatrix} b_{ci0} & b_{ci1} & ... & b_{cin} \\ b_{si0} & b_{si1} & ... & b_{sin} \end{bmatrix}$, and $i = 1, ..., N$.

Now since the trajectory parameters are point to point motions with zero initial position error and zero initial velocity, acceleration and jerk, therefore

the resulting e, Eqn. (4.21), as the system closely tracks the selected trajectory pattern will have the same harmonic content as in the right hand side of the error equation expressed by Eqn. (4.22). Thus, the resulting tracking error can be expressed as

$$e = E_0 + \sum_{i=1}^{N} \left[E_{ci} \cos\left(i\omega t + \phi_i\right) + E_{si} \sin\left(i\omega t + \phi_i\right) \right] \tag{3.18}$$

in which the amplitudes $E_0 = 0$ and E_{ci} and E_{si} are linear functions of the errors in the estimated values of the system parameters, i.e., Δm and Δk_j in the present system described by Eqn. (4.1), and the phase shift ϕ_i that can be readily seen to be given as

$$\phi_i = \arctan \frac{G_1 i\omega}{G_2 - m(i\omega)^2} \tag{3.19}$$

However, since with the initial trajectory parameters that yield relatively slow and small point to point motions the controller gains can be set to be relatively large, the resulting phase shifts can be made to be negligible, i.e., we can consider $\phi_i = 0$, where $i = 1, 2, ...N$. It is also noted that as the present parameter identification proceeds with larger trajectory parameters, the controller gains can still be set to be relatively large since the error in the system parameters would also become increasingly smaller.

The amplitudes E_0, E_{ci} and E_{si} in Eqn. (4.24) can be expressed as

$$\begin{aligned} E_0 &= T_0 a_0 \\ E_{\_i} &= T_i a_{\_i} \end{aligned} \tag{3.20}$$

where $T_0 = -\frac{1}{G_2}$, $T_i = -\frac{1}{\sqrt{i^2\omega^2 G_1^2 + (i^2\omega^2 m + G_2)^2}}$, and $i = 1, ..., N$.

Now by substituting a_0, a_{ci} and a_{si} from Eqn. (3.17) into Eqn. (4.26), the amplitudes E_0, E_{ci} and E_{si} can be shown to become

$$\begin{aligned}
\begin{bmatrix} E_0 \end{bmatrix} &= T_0 \mathbf{B}_0 \begin{bmatrix} \lambda\omega^2 & 0 & ... & 0 \\ 0 & \lambda^{p_1+q_1}\omega^{q_1} & ... & 0 \\ ... & ... & ... & ... \\ 0 & 0 & ... & \lambda^{p_n+q_n}\omega^{q_n} \end{bmatrix} \begin{bmatrix} \Delta m \\ \Delta k_1 \\ ... \\ \Delta k_n \end{bmatrix} \\
\begin{bmatrix} E_{ci} \\ E_{si} \end{bmatrix} &= T_i \mathbf{B}_i \begin{bmatrix} \lambda\omega^2 & 0 & ... & 0 \\ 0 & \lambda^{p_1+q_1}\omega^{q_1} & ... & 0 \\ ... & ... & ... & ... \\ 0 & 0 & ... & \lambda^{p_n+q_n}\omega^{q_n} \end{bmatrix} \begin{bmatrix} \Delta m \\ \Delta k_1 \\ ... \\ \Delta k_n \end{bmatrix}
\end{aligned} \tag{3.21}$$

As can seen from Eqn. (4.27), the amplitudes E_0, E_{ci} and E_{si} of the error harmonics are linear functions of the errors in the estimated values of the system parameters, i.e., Δm and Δk_j in the present system described by Eqn. (4.1).

Now let the vector $\bar{E} = [E_0, E_{c1}, E_{s1}, ...]^T$ represent the amplitudes of the error harmonics, Eqn. (4.24), and the vector $\bar{P} = [\Delta m, \Delta k_1, \Delta k_2, ...]^T$ represent the aforementioned errors in the estimated values of the system parameters, Eqn. (4.1). From Eqn. (4.27), the vectors $\bar{E}$ and $\bar{P}$ are therefore related by a matrix $\mathbf{M}$ as

$$\bar{E} = \mathbf{M}\bar{P} \tag{3.22}$$

where

$$\mathbf{M} = \begin{bmatrix} T_0 & 0 & ... & 0 \\ 0 & T_1 & ... & 0 \\ ... & ... & ... & ... \\ 0 & 0 & ... & T_N \end{bmatrix} \begin{bmatrix} \mathbf{B}_0 \\ \mathbf{B}_1 \\ ... \\ \mathbf{B}_N \end{bmatrix} \begin{bmatrix} \lambda\omega^2 & 0 & ... & 0 \\ 0 & \lambda^{p_1+q_1}\omega^{q_1} & ... & 0 \\ ... & ... & ... & ... \\ 0 & 0 & ... & \lambda^{p_n+q_n}\omega^{q_n} \end{bmatrix} \tag{3.23}$$

It is readily shown that the matrix $\mathbf{M}$ is the product of the indicated three matrices. The left matrix is diagonal with each term corresponding to the response amplitude to each error frequency. These terms are therefore also functions of the fundamental frequency ω and gains G_1, G_2 as indicated by Eqn. (4.26). The elements in the middle matrix are constant for a given system and selected trajectory pattern, Eqns. (4.23). And the right matrix is also diagonal and in tems of the known trajectory parameters.

It is noted that the elements of the left matrix on the right hand side of Eqn. (3.23) contain the gains G_1 and G_2, which may not be known precisely, as well as the system parameter m. As a result, the estimator matrix $\mathbf{M}$ cannot be calculated directly. However, for a given trajectory parameter ω and for a gain settings G_1 and G_2, the estimator matrix $\mathbf{M}$ is constant. Thus, Eqn. (4.29) can be used to calculate the elements of the estimator matrix $\mathbf{M}$ experimentally by measuring the error amplitudes $\bar{E}$ for different trajectory parameters λ and/or different system parameter correction vectors $\bar{P} = [\Delta m, \Delta k_1, \Delta k_2, ...]^T$.

Once the matrix $\mathbf{M}$ is known for a given set of trajectory parameters, the linear relationship in Eqn. (4.29) can be applied to the measured error vector $\bar{E}$ to calculate errors in the system parameters given by the vector

$\bar{P}$ as $\bar{P} = \mathbf{M}^{+}\bar{E}$, where $\mathbf{M}^{+}$ is any proper pseudo inverse operator (Moore-Penrose for example). The system parameters can then updated and the system parameter identification process continued with larger point-to-point motions, i.e., larger λ, and/or faster motions, i.e., larger ω.

It is noted that in practice, due to the measurement and rounding error during the calculations and noise, for the same trajectory parameters and gains, we may need to update system parameters and repeat the identification procedure until the convergence of their values within an appropriate range. It is also important to note that for a given set of trajectory parameters and controller gains, as the system parameters are identified more accurately the elements of the measured errors vector $\bar{E}$ diminishes, and becomes difficult and/or impossible to measure. At which point, we have to either increase the point-to-point motions, i.e., λ, or its speed, i.e., ω, or decrease the controller gains to increase the amplitudes of the measured errors, $\bar{E}$, and make it possible to more accurately identify the system parameters associated with the higher order dynamics of the system.

It is also noted that the matrix $\mathbf{M}$ is a linear map from the n dimensional vector space $\bar{P}$ to the $2N+1$ dimensional vector space $\bar{E}$ with $2N+1 > n$. Therefore, there are at most n numbers of linear independent harmonic amplitudes in the vector $\bar{E}$. If $\mathbf{M}'$ is a full rank n by n sub-matrix of the matrix $\mathbf{M}$ relating n linearly independent amplitudes in the measured error harmonic amplitudes (an n dimensional sub-vector $\bar{E}'$ of $\bar{E}$), since $\bar{E}' = \mathbf{M}'\bar{P}$, by only measuring the error harmonic amplitudes $\bar{E}'$, the error in estimated parameters $\bar{P}$ can be calculated. The sub-matrix $\mathbf{M}'$ may also be obtained as was previously described for the matrix $\mathbf{M}$.

The relationship Eqn. (4.29) can be used to develop a systematic process for the identification of the parameters of fully controlled nonlinear dynamics systems. In this process, with an initial estimated values of the system parameters that do not have to be accurate, the system is forced to track the trajectory pattern, Eqn. (4.13), starting with relatively small total point-to-point steps (small λ) and relatively slow motions (small ω) to ensure stability and relatively accurate tracking of the trajectory pattern. The tracking error e is then measured, and the amplitudes of its harmonics (i.e., the vector $\bar{E}$) are calculated using Fourier integration. Eqn. (4.29) is then used to calculate errors in the estimated values of the system parameters (Δm and Δk_j) for the system described by Eqn. (4.1). The model parameters are then updated and the process is repeated while slowly increasing the trajectory parameters λ and ω until the values of the system parameters, particularly those related to the higher order dynamics of the system are determined with enough accuracy.

The following general steps should be used to develop the model parameter identification algorithms based on the present method

Step 1:

Substitute the selected trajectory pattern (preferably of the form described by Eqn. (4.13)) into the differential equations of motion of the system to derive the relationship between the errors in the amplitudes of the N harmonics present in the control system generated errors $\bar{E}$ and the errors in the estimated values of the system parameters $\bar{P}$, Eqn. (4.29).

Step 2:

Make as good an estimate for the system parameter values as possible. Then depending on how good these estimates could be expected to be, select rel-

atively small values for the trajectory parameters. In general, when errors in the system parameter values are expected to be high, then smaller values are selected for the trajectory parameters to ensure stability during the initial trajectory tracking experiments.

Step 3:

For the given trajectory pattern, the error generated by the system controller is then measured and the amplitudes of its harmonics are calculated and used in Eqn. (4.29) to calculate the corrections Δm and Δk_j that should be made to the estimated values of the system parameters.

Step 4:

The experiment is repeated with the updated values of the system parameters. If the magnitudes of the amplitudes of the significant harmonics of the error generated by the system controller are small enough (according to preselected convergence limits), then go to Step 5. Otherwise, go back to Step 3.

Step 5:

If the magnitudes of all the significant harmonics N of the error generated by the system controller are small (according to the preselected convergence limits), and all the parameters to be identified have converged, the parameter estimation process is completed. Otherwise, increase the trajectory parameters (larger λ and/or ω, Eqn. (4.13)) and go to Step 3.

It is noted that in this parameter identification process, when the trajectory pattern parameters are small, the errors in the system parameters that contribute most to the lower harmonics of the system actuation forces/torques (and the tracking error) are mostly estimated. Then as longer paths, i.e., larger values of λ, and faster motions, i.e., higher fundamental frequency ω, are used,

the system parameters that contribute more to the higher order dynamics of the system are identified.

It is noted that the (estimator) matrix $\mathbf{M}$ is not usually square. Thus in the aforementioned system parameter identification process one has to use an appropriate method such as a least square algorithm.

It is also noted that the estimator matrix $\mathbf{M}$ is preferably derived analytically, particularly when the system dynamics are highly nonlinear. It is, however, also possible to determine the elements of the estimator matrix $\mathbf{M}$ experimentally. The latter method is obviously very straight forward and only requires results of two consecutive error harmonic amplitude measurements and linear interpolation. The elements of the estimator matrix $\mathbf{M}$ may then be updated as the system parameter identification process proceeds. The analytically derived estimator matrix $\mathbf{M}$ is also updated as the system parameter identification process proceeds. The analytical formulation of the estimator matrix is obviously preferred since not all the elements of the matrix are independent.

The details of the process of applying the developed nonlinear system parameter identification method is better described through the following example.

3.3 Example

Consider the fully controlled nonlinear dynamics system described by the differential equation of motion

$$m\ddot{x} + k_1 x + k_2 \dot{x}^2 = u \tag{3.24}$$

where m, k_1 and k_2 are the system parameters to be identified; x is the system output and u is the system input. The trajectory pattern Eqn. (4.13) is used in the present parameter identification process.

By applying Eqn. (3.11), we get the expanded polynomial form of the system as

$$m\ddot{e} + k_1 e + k_2 \dot{e}^2 + 2k_2 \dot{e}\dot{x}_r = \Delta m\ddot{x}_r + \Delta k_1 x_r + \Delta k_2 \dot{x}_r^2 + G_1\dot{e} + G_2 e \tag{3.25}$$

Substituting the trajectory pattern, Eqn. (4.13), into Eqn. (4.43) and rearranging into harmonic form, we get

$$\begin{aligned} m\ddot{e} \;-\; & G_1\dot{e} - G_2 e = \Delta m\ddot{x}_r + \Delta k_2 \dot{x}_r^2 + \Delta k_1 x_r = \frac{5}{9}\lambda^2\omega^2\Delta k_2 \\ +\; & (\lambda\Delta k_1 - \lambda\omega^2\Delta m)\cos\omega t - \frac{5}{6}\lambda^2\omega^2\Delta k_2 \cos 2\omega t \\ -\; & (\frac{1}{9}\lambda\Delta k_1 - \lambda\omega^2\Delta m)\cos 3\omega t + \frac{1}{3}\lambda^2\omega^2\Delta k_2 \cos 4\omega t \\ -\; & \frac{1}{18}\lambda^2\omega^2\Delta k_2 \cos 6\omega t \end{aligned} \tag{3.26}$$

During the identification, the error e between the actual and planned posi-

tions x_a and x_r, respectively, of the system is measured as a function of time, shown in Figure 3.1.

Fourier integration is then used to calculate the amplitudes of the harmonics with the fundamental frequency ω present in the measured error.

As mentioned previously, the output error vector can be defined as $\bar{E} = [E_0, E_{1c}, E_{2c}, E_{3c}, E_{4c}, E_{6c},]^T$, and the error vector in the estimated values of the system parameter be $\bar{P} = [\Delta m, \Delta k_1, \Delta k_2]^T$

The estimator matrix $\mathbf{M}$, Eqn. (4.29), is determined from Eqn. (4.25)-Eqn. (4.29) as

$$\mathbf{M} = \begin{bmatrix} T_0 & 0 & ... & 0 \\ 0 & T_1 & ... & 0 \\ ... & ... & ... & ... \\ 0 & 0 & ... & T_6 \end{bmatrix} \begin{bmatrix} 0 & 0 & \frac{5}{9} \\ -1 & 1 & 0 \\ 0 & 0 & -\frac{5}{6} \\ 1 & -\frac{1}{9} & 0 \\ 0 & 0 & \frac{1}{3} \\ 0 & 0 & -\frac{1}{18} \end{bmatrix} \begin{bmatrix} \lambda\omega^2 & 0 & 0 \\ 0 & \lambda & 0 \\ 0 & 0 & \lambda^2\omega^2 \end{bmatrix} \tag{3.27}$$

By relating small changes in the parameters being estimated to small changes in amplitude of error harmonics, a function mapping small changes in the parameter values to that of amplitudes of the error harmonics, $\bar{\mathbf{M}}$, is obtained. First, from the initially guessed system parameters $\bar{P}$, we measure the error e and calculated its harmonics $\bar{E}$. Next, from the initialed guessed parameters $\bar{P}$, we propose three parameters with small changes, $\bar{P}_1 = \bar{P} + [\delta m, 0, 0]^T$, $\bar{P}_2 = \bar{P} + [0, \delta k_1, 0]^T$, and $\bar{P}_3 = \bar{P} + [0, 0, \delta k_2]^T$, and then repeat the test to get three corresponding error vectors $\bar{E}_1$, $\bar{E}_2$, and $\bar{E}_3$. The matrix $\bar{\mathbf{M}}$ can be

obtained as

$$\bar{\mathbf{M}} = \left[\begin{array}{c|c|c} \frac{1}{\delta m}\left(\bar{E}_1 - \bar{E}\right) & \frac{1}{\delta k_1}\left(\bar{E}_2 - \bar{E}\right) & \frac{1}{\delta k_2}\left(\bar{E}_3 - \bar{E}\right) \end{array} \right] \tag{3.28}$$

And then the system parameters can be identified by $\bar{P} = \bar{\mathbf{M}}^{+}\bar{E}$.

It is noted that in this case, there are only three components in $\bar{E}$ that are linearly independent. Therefore, by defining them in a new vector $\bar{E}' = [E_0, E_{1c}, E_{3c}]^T$, a new estimator matrix $\mathbf{M}'$, which is full rank 3 by 3 in dimension, can be determined as

$$\mathbf{M}' = \begin{bmatrix} T_0 & 0 & 0 \\ 0 & T_1 & 0 \\ 0 & 0 & T_3 \end{bmatrix} \begin{bmatrix} 0 & 0 & \frac{5}{9} \\ -1 & 1 & 0 \\ 1 & -\frac{1}{9} & 0 \end{bmatrix} \begin{bmatrix} \lambda\omega^2 & 0 & 0 \\ 0 & \lambda & 0 \\ 0 & 0 & \lambda^2\omega^2 \end{bmatrix} \tag{3.29}$$

And then the system is identified by $\bar{P} = \bar{\mathbf{M}}'^{-1}\bar{E}'$, where the matrix $\bar{\mathbf{M}}'$ can be obtained with the same method as was described for $\bar{\mathbf{M}}$.

In both cases, the elements of the estimator matrix are updated following each parameter error identification run.

3.4 Conclusions

A new method for model parameter estimation of linear-in-the-parameters and fully controlled nonlinear dynamics systems such as robot manipulators with rigid links is presented and the mathematical proof of its stability and convergence is provided. The method is based on the Trajectory Pattern Method. In this method, for a pattern of motion the inverse dynamics model of the sys-

tem is derived in algebraic form in terms of the trajectory pattern parameters. The system dynamics model parameters are then identified using a systematic algorithm which ensures system stability as well as accurate estimation of the model parameters associated with lower as well as higher order dynamic terms. The method is shown to be fast converging and does not require initial close estimation of system parameters in order to ensure convergence.

Linear-in-the-parameters and fully controlled nonlinear dynamics systems constitute a very large class of practical dynamics systems such as robot manipulators and other computer controlled machinery, particularly high-speed and precision machines that are constructed with relatively rigid links and operate at speeds that are well below the first natural mode of vibration of the system.

It is noted that the main emphasis of the chapter has been in presenting the developed method and not the development of the optimal method of its implementation. For example, the use of Moore-Penrose pseudo-inverse matrix to resolve redundancy in the estimator matrix relationship Eqn. (4.29) can be significantly improved considering the generally smaller amplitudes but higher frequencies of the higher harmonic components of the measured error. In practice, the error rate (velocity) may also be measured and similarly used in the parameter identification process, particularly to achieve better measurement noise rejection.

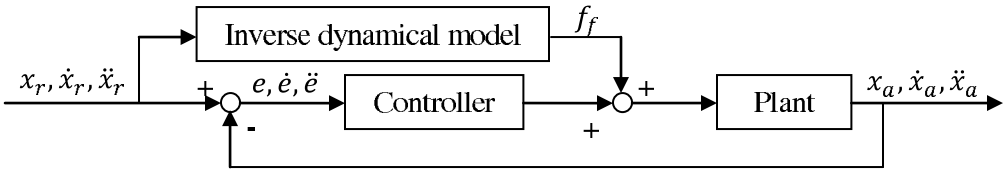

Figure 3.1: Feedforward Control System For Parameter Identification.

Chapter 4

Model Parameter Identification for None-Fully Controlled Nonlinear Dynamic System

4.1 Introduction

The dynamics of machines such as robot manipulators and those constructed with linkage mechanisms, particularly those operating at relatively high speeds, is highly nonlinear. The flexibility of links or joints, which construct such mechanical systems, introduces non-fully controlled complexity. The dynamics of such mechanical systems can be modeled as ordinary differential equations that are linear-in-parameters. Such models accurately represent a large class of mechanical systems and usually employ appropriate actuation and controls to form non-fully controlled nonlinear dynamics systems.

Identification of the model parameters of such systems such as their kine-

matics and dynamics (inertia) parameters is important for accurate prediction of the dynamic behavior of the system, for the design of the system, path and trajectory planning and synthesis, and their control (e.g., see [13]). In particular, accurate identification of model parameters is essential for the control of high-speed and ultra-precision machines, especially when model-based methods are required to achieve the desired system performance.

A number of investigators have developed procedures for the identification and calibration of the kinematics parameters of various mechanical systems, e.g., Ibarra and Perreira [14], Kazerounian and Qian [15], Goswami and Bosnik [16], Kaizerman, et al. [17] and Zak, et al. [18]. Others have contributed to the development of dynamics parameter identification techniques. For example, Guo and Angeles [19] developed a method for linearized systems for on-line recursive least square parameter estimation for feedback gains. Kawasaki and Nishimura [20] developed a method called "instrument variable method" (IVM) which yields more accurate estimation than least square methods (LSM). Based on a statistical framework, Swevers, et al. [21] formulated a maximum-likelihood estimation method for the dynamics parameters of robot models. Lin [22] developed a method which does not require the symbolic dynamics equations to identify the inertia parameters of a manipulator. In another study, Lin [23] showed an approach to identify the parameters of a manipulator based on the least square method. Dolanc and Strmcnik [24] used a piecewise-linear Hammerstein excitation signal for parameter estimation of nonlinear systems. Kenne, et al. [25] employed radial basis function networks for time varying parameter estimation of nonlinear systems. Spottswood and Allemang [26] proposed a frequency domain approach called "Modified Feed-

back of the Output Method" for parameter identification of reduced order nonlinear models.

Other related research has been in the area of the development of methods to identify the structure of appropriate models for nonlinear dynamics systems, including the present linear-in-parameters systems. For example, Li, et al. [27] developed a two-stage algorithm for identification of the structure of nonlinear dynamics systems in which an initial model is built from a large pool of basis functions or model terms and the significance of each term is evaluated. Gray, et al. [28] used a similar method together with Genetic Programming for nonlinear model structure identification. This method is an optimization method which automatically selects model structure elements from a database. Abdelazim and Malik [29] used a fuzzy logic grey box modeling technique for identification of the structure of nonlinear dynamics systems. Other published literature in the area of parameter identification for nonlinear linear-in-the-parameters dynamics system includes those Chen, et al. [30], Poroddi and Spinelli [31], and Zhu and Billings [32].

A review of the published literature indicates that a systematic method for parameter identification of highly nonlinear, non-fully controlled and linear-in-parameter mechanical systems such as robot manipulators or other similar computer controlled machines constructed with flexible structure, particularly if they are desired to operate at high-speeds with very high precision has not yet been developed. Such a method is required to guarantee that the system stays stable at all times during the identification process and that it can accurately identify parameters that contribute to the higher order dynamics terms, particularly those that become significant at higher operating speeds.

In this chapter, the development of such a method is presented. The method is based on the Trajectory Pattern Method [13, 33–40]. The method is robust and is applicable to highly nonlinear and non-fully controlled dynamics systems and does not require accurate initial estimation of the system parameters. The mathematical proof of the developed method is provided together with an example of its implementation on a nonlinear non-fully controlled dynamics system.

4.2 Model Parameter Identification Method

In this section, the developed systematic method for identification of the parameters of a class of non-fully controlled nonlinear dynamics systems such as serial robot manipulators with flexible links or joints is described and the mathematical proof of its convergence and stability during the identification process is provided. The dynamics of such systems are decoupled and described by ordinary differential equations in the form of so-called linear-in-the-parameters nonlinear systems as [27]

$$m_1\ddot{x}_1 + D(x_1, x_2, \dot{x}_1, \dot{x}_2, k_{11}, k_{12}, ..., k_{1n}) = u \tag{4.1}$$

$$m_2\ddot{x}_2 + k_{21}x_2 + k_{22}x_1 = 0 \tag{4.2}$$

$$m_3\ddot{x}_3 + k_{31}x_3 + k_{32}x_2 = 0 \tag{4.3}$$

$$...$$

$$m_l\ddot{x}_l + k_{l1}x_l + k_{l2}x_{l-1} = 0 \tag{4.4}$$

where x_1 is the controlled system output, x_2, x_3,..., x_l are non-controlled system output, u is the system input (control), and m_1, m_2,...,m_l, k_{11}, k_{12},..., k_{1n}, k_{21}, k_{22}, ..., k_{l1}, k_{l2} are the system parameters to be identified.

It is readily shown that the nonlinear term D in Eqn. (4.1) can be accurately expressed in polynomial form using Taylor series as shown in [13, 33–40] for robot manipulators with serial rigid links. The nonlinear term D can thereby be expressed in the following form

$$D(x_1, x_2, \dot{x}_1, \dot{x}_2, k_{11}, k_{12}, ..., k_{1n}) = \sum_{j=1}^{n} k_{1j} x_1^{p_{1j}} \dot{x}_1^{q_{1j}} x_2^{p_{2j}} \dot{x}_2^{q_{2j}} \tag{4.5}$$

where p_{1j}, q_{1j}, p_{2j} and q_{2j} are non-negative integer exponents of x_1, $\dot{x}_1$, x_2 and $\dot{x}_2$, respectively, in the jth term of the polynomial.

The vibration equations Eqn. (4.2), Eqn. (4.3), and Eqn. (4.4) can be rewritten as

$$x_1 = -\frac{m_2 \ddot{x}_2 + k_{21} x_2}{k_{22}} \tag{4.6}$$

$$x_2 = -\frac{m_3 \ddot{x}_3 + k_{31} x_3}{k_{32}} \tag{4.7}$$

$$...$$

$$x_{l-1} = -\frac{m_l \ddot{x}_l + k_{l1} x_l}{k_{l2}} \tag{4.8}$$

Solved from Eqn. (4.6), Eqn. (4.7), and Eqn. (4.8), we can get

$$x_1 = \sum_{i=0}^{l-1} r_{1i} x_l^{(2i)} \tag{4.9}$$

$$x_2 = \sum_{i=0}^{l-2} r_{2i} x_l^{(2i)} \tag{4.10}$$

where r_{1i}, r_{2i} are solved coefficients from the elimination of equations, $x_l^{(2i)}$ is the $2i$ order derivative of x_l.

Substitute Eqn. (4.9) and Eqn. (4.10) into Eqn. (4.5), let $x = x_l$, and then Eqn. (4.1) can be rewritten as a new high order fully controlled dynamics system

$$c_1 x^{(2l)} + D_1(x, \dot{x}, \ddot{x}, ..., x^{(2l-1)}, c_2, c_3, c_4, ...c_{n'}) = u \tag{4.11}$$

where D_1 is a new nonlinear term in polynomial form

$$\begin{aligned} &D_1(x, \dot{x}, \ddot{x}, ..., x^{(2l-1)}, c_2, c_3, c_4, ...c_{n'}) = \\ &\sum_{j=1}^{n'-1} c_{j+1} x^{p_{1j}} \dot{x}^{p_{2j}} \ddot{x}^{p_{3j}} ... (x^{(2l-1)})^{p_{(2l)j}} \end{aligned} \tag{4.12}$$

where p_{1j}, p_{2j}, ... $p_{(2l)j}$ are non-negtive integar exponents of x, $\dot{x}$, $\ddot{x}$, ..., $x^{(2l-1)}$, respectively, in the jth term of the polynomial and c_{j+1} is the coefficient of such term, which are also the parameters of the new linear-in-parameter dynamics system. The totally n' numbers parameters, c_1, c_2, ...$c_{n'}$, can be analytically derived from the system parameters m_1, m_2,... . Therefore the system parameters can be obtained after identifying the n' number of parameters from the new system, Eqn. (4.11).

Now consider the trajectory pattern

$$x_r = \lambda \left[\cos(\omega t) + \sum_{i=1}^{l-1} a_i \cos(2i+1)\omega t \right] \tag{4.13}$$

where x_r is the desired motion, ω is the fundamental frequency of the trajectory and one of the trajectory parameters, λ is the other trajectory parameter

and a_i are the amplitude of harmonic components to ensure $\dot{x}_r(0) = \ddot{x}_r(0) = ... = x_r^{(2l+1)}(0) = \dot{x}_r(\pi/\omega) = \ddot{x}_r(\pi/\omega) = ... = x_r^{(2l+1)}(\pi/\omega) = 0$. With the motion starting at time $t = 0$ and ending at time $t = \pi/\omega$, i.e., half the period of the fundamental frequency ω, this trajectory pattern provides smooth point-to-point motions with zero initial and final velocity, acceleration and jerk for all outputs x_1, x_2, ...,x_l[**?**]. In this trajectory pattern, the time to complete the point-to-point motion is determined by the trajectory parameter (fundamental frequency) ω, and the trajectory parameter λ indicates the total distance traveled during the motion. The trajectory pattern (4.13) has low harmonic content, thereby is suitable for synthesizing point-to-point motions in nonlinear dynamics systems since it can be expected to demand low actuating force/torque harmonics. As a result, lower dynamic response is generally required from the actuation devices as compared to arbitrarily synthesized trajectories. The fundamental frequency ω can also be selected such that the natural modes of vibration of the system are not excited in resonance during the motion.

In the present method, a feed-forward control system with a linear feedback loop such as the one shown in Figure 3.1 is used to achieve full system control. The feed-forward signal f_f is calculated from the inverse dynamics model of the system, Eqn. (4.11), with the estimated system parameters c_1, c_2,..., $c_{n'}$. The feedback gains of the linear controller are considered to be large enough to achieve accurate trajectory tracking. It is shown later in this section that with the trajectory pattern Eqn. (4.13) and by selecting appropriate values for the trajectory parameters ω and λ, any nonlinear dynamics system of the form Eqn. (4.11) can be forced to accurately follow the synthesized trajectory

with an appropriately designed actuation device and a linear feedback control with high enough gains.

For the trajectory pattern Eqn. (4.13) the feed-forward signal f_f, Figure 3.1, is calculated from the dynamics model of the system, Eqn. (4.11). Since the system parameters are not yet unknown, their estimated values, denoted here as c'_1 , c'_2 ,..., $c'_{n'}$ are used to calculate the feed-forward signal as

$$f_f = c'_1 x_r^{(2l)} + D_1(x_r, \dot{x}_r, \ddot{x}_r, ..., x_r^{(2l-1)}, c'_2, c'_3, c'_4, ...c'_{n'}) \tag{4.14}$$

The control loop dynamics, Figure 3.1, can be described by

$$c_1 x_a^{(2l)} + D_1(x_a, \dot{x}_a, \ddot{x}_a, ..., x_a^{(2l-1)}, c_2, c_3, c_4, ...c_{n'}) = f_f + C(e) \tag{4.15}$$

where $C(e)$ is the control signal and e is the error $e = x_a - x_r$, where x_a is the system output. Substituting x_a with $x_r + e$ in Eqn. (4.15), we get

$$\begin{aligned} c_1 e^{(2l)} + c_1 x_r^{(2l)} + \quad D_1 \quad & (x_r + e, \dot{x}_r + \dot{e}, \ddot{x}_r + \ddot{e}, ..., x_r^{(2l-1)} + e^{(2l-1)}, \\ & c_2, c_3, c_4, ...c_{n'}) = f_f + C(e) \end{aligned} \tag{4.16}$$

However, since D_1 in Eqn. (4.16) is a polynomial function, it can be rearranged

into the following form

$$
\begin{aligned}
& D_1(x_r + e, \dot{x}_r + \dot{e}, \ddot{x}_r + \ddot{e}, ..., x_r^{(2l-1)} + e^{(2l-1)}, c_2, c_3, c_4, ...c_{n'}) \\
& = D_1(x_r, \dot{x}_r, \ddot{x}_r, ..., x_r^{(2l-1)}, c_2, c_3, c_4, ...c_{n'}) \\
& + D_1(e, \dot{e}, \ddot{e}, ..., e^{(2l-1)}, c_2, c_3, c_4, ...c_{n'}) \\
& + D_1'(x_r, \dot{x}_r, \ddot{x}_r, ..., x_r^{(2l-1)}, e, \dot{e}, \ddot{e}, ..., e^{(2l-1)}, c_2, c_3, c_4, ...c_{n'})
\end{aligned}
\tag{4.17}
$$

where the term D_1' is another polynomial function whose order is one less than the term D_1. By substituting Eqn. (4.17) and Eqn. (4.14) into Eqn. (4.16) and rearranging the resulting equation, we get

$$
\begin{aligned}
c_1 e^{(2l)} \quad + \quad & D_1(e, \dot{e}, \ddot{e}, ..., e^{(2l-1)}, c_2, c_3, c_4, ...c_{n'}) + \\
& D_1'(x_r, \dot{x}_r, \ddot{x}_r, ..., x_r^{(2l-1)}, e, \dot{e}, \ddot{e}, ..., e^{(2l-1)}, c_2, c_3, c_4, ...c_{n'}) \\
= \quad & c_1' x_r^{2l} - c_1 x_r^{2l} + D_1(x_r, \dot{x}_r, \ddot{x}_r, ..., x_r^{(2l-1)}, c_2', c_3', c_4', ...c_{n'}') \\
& - D_1(x_r, \dot{x}_r, \ddot{x}_r, ..., x_r^{(2l-1)}, c_2, c_3, c_4, ...c_{n'}) + C(e)
\end{aligned}
\tag{4.18}
$$

Since the terms D_1 and D_1' are polynomial functions in which the parameters $c_i s$ and $c_i' s$ are coefficients of the polynomial terms, therefore the functions D and D' are linear with respect to the parameters $c_i s$ and $c_i' s$. The first four terms on the right hand side of the Eqn. (4.18) can be written in the following

simplified form

$$\begin{aligned} c_1' x_r^{2l} &- c_1 x_r^{2l} + D_1(x_r, \dot{x}_r, \ddot{x}_r, ..., x_r^{(2l-1)}, c_2', c_3', c_4', ...c_{n'}') \\ &- D_1(x_r, \dot{x}_r, \ddot{x}_r, ..., x_r^{(2l-1)}, c_2, c_3, c_4, ...c_{n'}) = \\ &\Delta c_1 x_r^{2l} + D_1(x_r, \dot{x}_r, \ddot{x}_r, ..., x_r^{(2l-1)}, c_2, c_3, c_4, ...c_{n'}) \end{aligned} \tag{4.19}$$

where $\Delta c_i = c_i' - c_i$ are errors in the estimated parameter values c_i, $i = 1, 2, ..., n'$.

By substituting Eqn. (4.19) into Eqn. (4.18), we get

$$\begin{aligned} c_1 e^{(2l)} &+ D_1(e, \dot{e}, \ddot{e}, ..., e^{(2l-1)}, c_2, c_3, c_4, ...c_{n'}) + \\ &D_1'(x_r, \dot{x}_r, \ddot{x}_r, ..., x_r^{(2l-1)}, e, \dot{e}, \ddot{e}, ..., e^{(2l-1)}, c_2, c_3, c_4, ...c_{n'}) \\ &= \Delta c_1 x_r^{2l} + D_1(x_r, \dot{x}_r, \ddot{x}_r, ..., x_r^{(2l-1)}, c_2, c_3, c_4, ...c_{n'}) + C(e) \end{aligned} \tag{4.20}$$

Now consider the use of a linear controller such as a PD controller $C(e) = G_1\dot{e} + G_2 e$, where G_1 and G_2 are the proportional and derivative gains with large enough values. By substituting the control signal $C(e)$ into the Eqn. (4.20) and rearranging by bringing all e and $\dot{e}$ terms to the left hand side. All their higher order terms of error can neglected since e terms can be forced to become very small by the selection of small trajectory parameters λ and ω and large enough controller gains, we get

$$-G_1\dot{e} - G_2 e = \Delta c_1 x_r^{(2l)} + \sum_{j=1}^{n'-1} \Delta c_{j+1} x_r^{p_{1j}} \dot{x}_r^{p_{2j}} \ddot{x}_r^{p_{3j}} ... (x_r^{(2l-1)})^{p_{(2l)j}} \tag{4.21}$$

As expected, with the assumption of small enough trajectory parameters λ and ω and large enough controller gains, the differential equation describing the error becomes linear. As can be observed, the requirement of close enough model parameter estimation in general feedforward control has been replaced by the requirement of small enough trajectory parameters λ and ω to ensure stability with closely approximated linear differential equation describing the system tracking error, Eqn. (4.21).

This means that by using the developed trajectory pattern method, the system parameters of non-fully controlled nonlinear dynamics systems such as robot manipulators with flexible links or joints can be identified without the availability of good estimated values for the system parameters as described below. By substituting the selected trajectory pattern Eqn. (4.13) into the right hand side of the Eqn. (4.21) and then expand to harmonics form, we get

$$\begin{aligned} \Delta c_1 x_r^{(2l)} + \sum_{j=1}^{n'-1} \Delta c_{j+1} x_r^{p_{1j}} \dot{x}_r^{p_{2j}} \ddot{x}_r^{p_{3j}} ... (x_r^{(2l-1)})^{p_{(2l)j}} \\ = a_0 + \sum_{i=1}^{N} \left[a_{ci} \cos(i\omega t) + a_{si} \sin(i\omega t) \right] \end{aligned} \tag{4.22}$$

where N is the highest harmonic component with significant amplitude present in the error as the system is forced to follow the trajectory pattern Eqn. (4.13).

Now as can be seen from the Eqn. (4.22), the amplitudes a_0, a_{ci} and a_{si} of the harmonics can be expressed as a linear combination of the errors in the estimated values of the system parameters, i.e., Δc_j in the present system described by the Eqn. (4.11). Thus, by defining $b_{\_ij}(\lambda, \omega)$ as polynomial functions of the trajectory parameters λ and ω (the underscore _ standing for

either s or c), the amplitudes $a_{\_i}$ can be expressed as

$$a_{\_i} = \sum_{j=0}^{n'} b_{\_ij}(\lambda, \omega)\Delta c_j \tag{4.23}$$

Now since the trajectory parameters are point to point motions with zero initial position error and zero velocity, acceleration and jerk, therefore the resulting error e, Eqn. (4.21), as the system closely tracks the selected trajectory pattern, will have the same harmonic pattern as the right hand side of the error equation expressed by the Eqn. (4.22). Thus, the resulting tracking error can be expresses as

$$e = E_0 + \sum_{i=1}^{N} \left[E_{ci} \cos(i\omega t) + E_{si} \sin(i\omega t)\right] \tag{4.24}$$

in which the amplitudes $E_0 = 0$ and E_{ci} and E_{si} are linear functions of the errors in the estimated values of the system parameters, i.e., Δc_j in the present system that is described by the Eqn. (4.11).

The linear differential equation describing the above tracking error Eqn. (4.21) generates a phase shift ϕ that can be readily seen to be given as

$$\phi = \arctan \frac{G_1 \omega}{G_2} \tag{4.25}$$

And the amplitudes E_{ci} and E_{si} can readily be shown to be described as

$$\begin{aligned} E_{ci} &= \frac{a_{ci} \cos\phi + a_{si} \sin\phi}{\sqrt{i^2\omega^2 G_1^2 + G_2^2}}, \\ E_{si} &= \frac{a_{si} \cos\phi + a_{ci} \sin\phi}{\sqrt{i^2\omega^2 G_1^2 + G_2^2}} \end{aligned} \tag{4.26}$$

Now by substituting a_{ci} and a_{si} from Eqn. (4.23) into Eqn. (4.26), the amplitudes E_{ci} and E_{si} can be shown to become

$$E_{ci} = \frac{\sum_{j=0}^{n} b_{cij}(\lambda,\omega)\Delta c_j}{\sqrt{i^2\omega^2 G_1^2 + G_2^2}} \cos\phi + \frac{\sum_{j=0}^{n} b_{sij}(\lambda,\omega)\Delta c_j}{\sqrt{i^2\omega^2 G_1^2 + G_2^2}} \sin\phi \tag{4.27}$$

$$E_{si} = \frac{\sum_{j=0}^{n} b_{sij}(\lambda,\omega)\Delta c_j}{\sqrt{i^2\omega^2 G_1^2 + G_2^2}} \cos\phi + \frac{\sum_{j=0}^{n} b_{cij}(\lambda,\omega)\Delta c_j}{\sqrt{i^2\omega^2 G_1^2 + G_2^2}} \sin\phi \tag{4.28}$$

As can seen from Eqn. (4.27) and Eqn. (4.28), the amplitudes E_{ci} and E_{si} of the error harmonics are linear functions of the errors in the estimated values of the system parameters, i.e., Δc_j, Eqn. (4.11).

Now let the vector $\bar{E} = [E_0, E_{1c}, E_{2c}, ...]^T$ represent the amplitudes of the error harmonics, Eqn. (4.24), and the vector $\bar{P} = [\Delta c_1, \Delta c_2, ...]^T$ represent the aforementioned errors in the estimated values of the system parameters, i.e., Δc_j in the present system that is described by the Eqn. (4.11). The vectors $\bar{E}$ and $\bar{P}$ are therefore related by an appropriately dimensioned matrix $\mathbf{M}$ as

$$\bar{E} = \mathbf{M} \times \bar{P} \tag{4.29}$$

The relationship Eqn. (4.29) can be used to develop a systematic process for the identification of the parameters of non-fully controlled nonlinear dynamics systems. In this process, with an initial estimated values of the system parameters (that do not have to be accurate), the system is forced to track

the trajectory parameter Eqn. (4.13) with small enough trajectory parameters to ensure stability and relatively accurate tracking of the trajectory pattern. The tracking error e is then measured, the amplitudes of its harmonics (i.e., the vector $\bar{E}$) are calculated using Fourier integration. The Eqn. (4.29) is then used to calculate errors in the estimated values of the system parameters, i.e., Δm and Δk_j. The model parameters are then updated and the process is repeated while slowly increasing the trajectory parameters, i.e., by increasing the length of the point to point motions λ and their speed of travel ω, until the values of the system parameters are determined with the desired level of accuracy.

The following general steps should be used to develop model parameter identification algorithms based on the present method:

Step 1:

Substitute the selected trajectory pattern (preferably of the form described by Eqn. (4.13)) into the differential equations of motion of the system to derive the relationship between the errors in the amplitudes of the N (significant) harmonics present in the control system generated errors $\bar{E}$ and the errors in the estimated values of the system parameters $\bar{P}$, Eqn. (4.29).

Step 2:

Make as good an estimate for the system parameter values as possible. Then depending on how good these estimates could be expected to be, select relatively small values for the trajectory parameters λ and ω. In general, when errors in the system parameter values are expected to be high, then smaller values are selected for the trajectory parameters to ensure stability during the initial trajectory tracking experiments.

Step 3:

For the given trajectory pattern, the error generated by the system controller is then measured and the amplitudes of its harmonics are calculated and used in the Eqn. (4.29) to calculate the corrections Δm and Δk_j that should be made to the estimated values of the system parameters.

Step 4:

The experiment is repeated with the updated values of the system parameters. If the magnitudes of the amplitudes of the significant harmonics of the error generated by the system controller are small enough (according to a preselected convergence limits), then go to the Step 5. Otherwise, go back to Step 4.

Step 5:

If the magnitudes of all significant harmonics N of the error generated by the system controller are small (according to a preselected convergence limits), the parameter estimation process is completed. Otherwise, increase the trajectory parameters, i.e., increase λ and/or ω, Eqn. (4.13), and go to the Step 3.

It is noted that in this parameter identification process, when the trajectory pattern parameters are small, the errors in the system parameters that contribute most to the lower harmonics of the system actuation forces/torques (and the tracking error) are generally better estimated. Then as the trajectory pattern parameters are made larger, i.e., as longer paths and faster motions are used, the better estimation are made of the errors in the system parameters that contribute to higher harmonics of the system actuation forces/torques, i.e., the system parameters corresponding to higher order terms of the system dynamics.

It is noted that the (estimator) matrix $\mathbf{M}$ is not usually square. Thus in

the aforementioned system parameter identification process one has to use an appropriate method such as one based on a least square algorithm to calculate system parameter corrections.

It is also noted that the estimator matrix $\mathbf{M}$ is preferably derived analytically, particularly when the system dynamics is highly nonlinear. It is, however, also possible to determine the elements of the estimator matrix $\mathbf{M}$ experimentally. The latter method is obviously very straight forward and only requires results of two consecutive error harmonic amplitude measurements and linear interpolation. The elements of the estimator matrix $\mathbf{M}$ may then be updated as the system parameter identification process proceeds. The analytically derived estimator matrix $\mathbf{M}$ is also updated as the system parameter identification process proceeds. The analytical formulation of the estimator matrix is obviously preferred since not all the elements of the matrix are independent.

The details of the process of applying the developed systematic nonlinear system parameter identification method are better described through the following example.

4.3 Example

Consider the non-fully controlled nonlinear dynamics system to be identified shown in Figure 4.1.Two carts m_1 and m_2 are connected by a linear spring with rate k_3 while cart m_1 is bounded to the ground via a nonlinear spring with rate $k(x) = k_1x + k_2x^3$. The control force F is applied on cart m_1, and cart m_2 is free. x_1 and x_2 are the system output. Such system can be described

by the differential equations of motion as

$$m_1\ddot{x}_1 + k_1x_1 + k_2x_1^3 + k_3(x_1 - x_2) = F \tag{4.30}$$

$$m_2\ddot{x}_2 + k_3(x_2 - x_1) = 0 \tag{4.31}$$

where m_1, m_2, k_1, k_2, k_3 are the system parameters to be identified; x_1 and x_2 are the system outputs and F is the system input. Such non-fully controlled dynamics system can be converted into a higher order fully controlled system, and then be identified with the presented method.

First solve x_1 from Eqn. (4.31)

$$x_1 = \frac{m_2}{k_3}\ddot{x}_2 + x_2 \tag{4.32}$$

And then substitute x_1 from Eqn.(4.32) into Eqn. (4.30), we have

$$\frac{m_1m_2}{k_3}\dddot{x}_2 + (m_1 + m_2)\ddot{x}_2 + k_1(\frac{m_2}{k_3}\ddot{x}_2 + x_2) + k_2(\frac{m_2}{k_3}\ddot{x}_2 + x_2)^3 = F \tag{4.33}$$

Rearrange Eqn. (4.33), we get an one degree of freedom linear-in-parameter fully controlled dynamics system to identify

$$c_1\ddddot{x}_2 + c_2\ddot{x}_2 + c_3\ddot{x}_2x_2^2 + c_4\ddot{x}_2^2x_2 + c_5\ddot{x}_2^3 + c_6x_2 + c_7x_2^3 = F \tag{4.34}$$

where

$$c_1 = \frac{m_1 m_2}{k_3} \tag{4.35}$$

$$c_2 = m_1 + m_2 + \frac{k_1 m_2}{k_3} \tag{4.36}$$

$$c_3 = \frac{3k_2 m_2}{k_3} \tag{4.37}$$

$$c_4 = \frac{3k_2 m_2^2}{k_3^2} \tag{4.38}$$

$$c_5 = \frac{k_2 m_2^3}{k_3^3} \tag{4.39}$$

$$c_6 = k_1 \tag{4.40}$$

$$c_7 = k_2 \tag{4.41}$$

Therefore by identifying parameters c_1 thru c_7, the system parameters m_1, m_2, k_1, k_2, k_3 can be obtained.

The trajectory pattern Eqn. (4.42) is synthesized as presented parameter identification process.

$$x_{2r} = \lambda \left(\cos \omega t - \frac{1}{6} \cos 3\omega t + \frac{1}{50} \cos 5\omega t \right) \tag{4.42}$$

By applying Eqn. (4.21), we get the expanding polynomial form of this system as

$$\begin{aligned} -G_1 \dot{e} - G_2 e = {} & \Delta c_1 \dddot{x}_{2r} + \Delta c_2 \ddot{x}_{2r} + \Delta c_3 \ddot{x}_{2r} x_{2r}^2 + \Delta c_4 \ddot{x}_{2r}^2 x_{2r} \\ & + \Delta c_5 \ddot{x}_{2r}^3 + \Delta c_6 x_{2r} + \Delta c_7 x_{2r}^3 \end{aligned} \tag{4.43}$$

Eqn. (4.25) shows the phase shifting of this system is $\phi = \arctan \frac{G_1 \omega}{G_2}$.

Without loss of generality, we choose the proportional controller to be dominating by set the gain $|G_2| \gg |\omega G_1|$. Such that the phase shifting $\phi \approx 0$, and then only cosine harmonics in the error are significant.

During the identification, the error e between the actual and planned positions x_{2a} and x_{2r}, respectively, of the system is measured as a function of time, Figure 3.1.

Fourier integration is then used to calculate the amplitudes of the harmonics with the fundamental frequency ω present in the measured error.

Let the amplitudes of the cosine part error harmonic vector be let the error vector be $\bar{E} = [E_{c1}, E_{c3}, E_{c5}, E_{c7}, E_{c9}, E_{c11}, E_{c13}, E_{c15}]^T$, and the aforementioned error vector in the estimated values of the system parameter be $\bar{P} = [\Delta c_1, \Delta c_2, ..., \Delta c_7]^T$.

The estimator matrix $\mathbf{M}$, Eqn. (4.29), is determined from Eqn. (4.25)-

Eqn. (4.28) as

$$M = -\frac{1}{G_2}\begin{bmatrix} \lambda\omega^4 & -\lambda\omega^2 & -\frac{92411}{180000}\lambda^3\omega^2 & \frac{533}{480}\lambda^3\omega^4 \\ -\frac{27}{2}\lambda\omega^4 & \frac{3}{2}\lambda\omega^2 & \frac{37393}{180000}\lambda^3\omega^2 & -\frac{877}{480}\lambda^3\omega^4 \\ \frac{25}{2}\lambda\omega^4 & -\frac{1}{2}\lambda\omega^2 & \frac{7973}{180000}\lambda^3\omega^2 & -\frac{1337}{2400}\lambda^3\omega^4 \\ 0 & 0 & -\frac{37373}{180000}\lambda^3\omega^2 & \frac{1183}{2400}\lambda^3\omega^4 \\ 0 & 0 & \frac{1273}{20000}\lambda^3\omega^2 & -\frac{1099}{2400}\lambda^3\omega^4 \\ 0 & 0 & -\frac{1993}{180000}\lambda^3\omega^2 & \frac{113}{800}\lambda^3\omega^4 \\ 0 & 0 & \frac{59}{60000}\lambda^3\omega^2 & -\frac{43}{2400}\lambda^3\omega^4 \\ 0 & 0 & -\frac{1}{20000}\lambda^3\omega^2 & \frac{1}{800}\lambda^3\omega^4 \end{bmatrix}$$

$$\begin{bmatrix} -\frac{99}{32}\lambda^3\omega^6 & \lambda & \frac{39761}{60000}\lambda^3 \\ \frac{187}{32}\lambda^3\omega^6 & -\frac{1}{6}\lambda & \frac{1157}{180000}\lambda^3 \\ -\frac{99}{32}\lambda^3\omega^6 & \frac{1}{50}\lambda & -\frac{109991}{1500000}\lambda^3 \\ -\frac{21}{32}\lambda^3\omega^6 & 0 & \frac{1847}{60000}\lambda^3 \\ \frac{57}{32}\lambda^3\omega^6 & 0 & -\frac{3163}{540000}\lambda^3 \\ -\frac{33}{32}\lambda^3\omega^6 & 0 & \frac{43}{60000}\lambda^3 \\ \frac{9}{32}\lambda^3\omega^6 & 0 & -\frac{1}{20000}\lambda^3 \\ -\frac{1}{32}\lambda^3\omega^6 & 0 & \frac{1}{500000}\lambda^3 \end{bmatrix} \tag{4.44}$$

Alternatively, the estimator matrix $\mathbf{M}$ is calculated from the Eqn. (4.26) by initially using a small change in the system parameter, Δc_1 to Δc_7, and calculating the corresponding changes in the amplitudes of the error harmonics.

In both cases, the elements of the estimator matrix $\mathbf{M}$ is updated following each parameter error identification run. In this example, since the estimator matrix $\mathbf{M}$ is not square, the Moore-Penrose pseudoinverse matrix is

used to solve for the errors in the system parameter values. Thus, if $\mathbf{M}^+$ is the Moore-Penrose pseudoinverse of the matrix $\mathbf{M}$, then the errors in the system parameter values $\bar{P}$ is given by $\bar{P} = \mathbf{M}^+ \times \bar{E}$, where $\bar{E}$ is the aforementioned vector of amplitudes of the harmonics present in the measured error e.

4.4 Conclusions

A new method for model parameter estimation of linear-in-the-parameters and non-fully controlled nonlinear dynamics systems such as robot manipulators with flexible links or joints is presented and its mathematical proof of its stability and convergence is provided. The method is based on the Trajectory Pattern Method. In this method, for a pattern of motion the inverse dynamics model of the system is derived in algebraic form in terms of the trajectory pattern parameters. The system dynamics model parameters are then identified using a systematic algorithm which ensures system stability as well as accurate estimation of the model parameters associated with lower as well as higher order dynamic terms. The method is shown to be fast converging and that does not require initial close estimation of system parameters in order to ensure convergence.

The linear-in-the-parameters and non-fully controlled nonlinear dynamics systems constitute a very large class of practical dynamics systems such as robot manipulators and other computer controlled machinery, particularly high-speed and precision machines that are constructed with flexible links or joints and operate at speeds that are well below the first natural mode of vibration of the system.

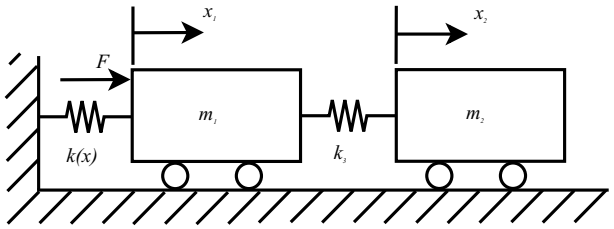

Figure 4.1: A 2-dof non-fully controlled dynamic ssystem

Chapter 5

Experiment and Method Validation

5.1 Introduction

In this chapter, an experiment is designed and executed to verify the parameter identification method. A highly nonlinear two degrees of freedom manipulator is built. The controller adopts Digital Signal Processor as real-time feedback/feedforward system and the velocity, position decoder is based on field-programmable gate array. The experiment follows the proposed procedure in chapter 3, and the result shows convergence of model parameter identification based on proposed method.

5.2 System Dynamics Equations of Motion

A two DOF closed loop planar manipulator is built for validating the presented parameter identification method, shown in Figure 5.1. The model parameters m_{12}, m_3,m_4, and m_{56} represent the masses of the four links; I_{12}, I_3,I_4, and I_{56} are the moments of inertia; l_1 through l_6 are the link lengths between joints; and r_1 through r_5 represent the distances from the joint to the centroid of the links.

θ_1, θ_2 are system output positions, and τ_1, τ_2 are system inputs. The differential equations of motion are

$$2f_1(\theta_2)\ddot{\theta_1} + f_3(\theta_2)\ddot{\theta_2} + 2\frac{df_1(\theta_2)}{d\theta_2}\dot{\theta_1}\dot{\theta_2} + \frac{df_3(\theta_2)}{d\theta_2}\dot{\theta_2}^2 = \tau_1 \quad (5.1)$$

$$f_3(\theta_2)\ddot{\theta_1} + 2f_2(\theta_2)\ddot{\theta_2} - \frac{df_1(\theta_2)}{d\theta_2}\dot{\theta_1}^2 + \frac{df_2(\theta_2)}{d\theta_2}\dot{\theta_2}^2 = \tau_2 \quad (5.2)$$

where $f_1(\theta_2)$, $f_2(\theta_2)$, and $f_3(\theta_2)$ are nonlinear functions of θ_2. The details of the definition are described in Appendix A.

The planned trajectory patterns for two outputs are

$$\theta_1 = \theta_{10} + \lambda_1(\cos\omega t - \frac{1}{9}\cos 3\omega t - \frac{8}{9}) \quad (5.3)$$

$$\theta_2 = \theta_{20} + \lambda_2(\cos\omega t - \frac{1}{9}\cos 3\omega t - \frac{8}{9}) \quad (5.4)$$

where θ_{10} and θ_{20} are the start position of the two outputs.

Therefore we can expand $f_1(\theta_2)$, $f_2(\theta_2)$, and $f_3(\theta_2)$ to the second order at the start position θ_{20}, and then the coefficients become the model parameters to identify. Refer to Appendix A for the relationship among those model

parameters.

$$f_1(\theta_2) = a_{10} + a_{11}(\theta_2 - \theta_{20}) + a_{12}(\theta_2 - \theta_{20})^2 \quad (5.5)$$

$$f_2(\theta_2) = a_{20} + a_{21}(\theta_2 - \theta_{20}) + a_{22}(\theta_2 - \theta_{20})^2 \quad (5.6)$$

$$f_3(\theta_2) = a_{30} + a_{31}(\theta_2 - \theta_{20}) + a_{32}(\theta_2 - \theta_{20})^2 \quad (5.7)$$

The expansions to the harmonic forms from the polynomial forms are described in Appendix B. The matrix $\mathbf{M}$ can then be constructed following the procedure of the last example.

5.3 Experiment Setup

The two degrees of freedom manipulator is built as shown in Figure. (5.2). Two AC brushless motors are mounted at joint 1 and 2 to generate input torque. Two incremental quadrature encoders mounted on the shafts of the motors are used for motion detection.

The control system is built as shown in Figure 5.3. A dell high performance workstation is the host computer. The GUI program, shown in Figure 5.4, downloads the estimated parameters onto a hosted 450MHz floating point TI 6713 DSP system to drive the manipulator using inverse dynamics feedforward. Such DSP system reads the actual position profile of joints from a high speed (50MHz clock) Xilinx Spartan III FPGA based logic circuit, which is built to decode the pulse signals from the encoders, debounce the noise, and then output the actual positions. IIR low pass filter and least square fitting algorithms are implemented in the DSP system for position

and velocity smoothing. From the error of position, the real time DSP sends feedback torque commands add to the feed-forward commands to the D/A converter, to compensate the error. Two power amplifiers, in torque/current mode, accept the analog command output from D/A converters, to drive the AC brushless motors. In the mean time, the DSP system communicates with the GUI program running in the workstation through a PCI-64 bus to report the error for data analysis and new parameter estimation.

The trajectory parameters for the initial cycle of the identification process are selected to be $\lambda_1 = -14.06°$, $\lambda_2 = 11.43°$ and $\omega = 2rad/s$. The controllers for the two motors are selected to be proportional controllers with gains of 6519 and 4237, which are selected using standard techniques to guarantee stability. The system parameters are unknown. The initial estimations for the system parameter values are poorly guessed and adjusted by observing the system outputs from several randomly picked numbers.

Following each model parameter identification run, the values of the trajectory pattern parameters are increased until the calculated errors in the system parameter values become small and fall within the desired convergence limit. Since the total trip for both motors are large enough in this experiment, we are going to increase only the fundamental frequency parameter of the trajectory pattern. And when the controller output signal reaches about 70% of the maximum allowed output level, the experiment is finished.

5.4 Procedure and Result

The matrix **M** is first calculated numerically with the aforementioned poor initial system parameter values and updated after each identification run. Before using the matrix to correct the error for the system parameters, the analytical matrix form is applied to regulate matrix **M** by clearing those entries which should be zero.

Table 5.1: System Parameter Identification Runs.

ω	a'_{10}	a'_{11}	a'_{12}	a'_{20}	$a_{21'}$	a'_{22}	a'_{30}	a'_{31}	a'_{32}
2	2281	1003	0	229	109	0	−1067	−474	0
2	2285	837	−11	215	173	88	−1061	−573	−46
2.6	2302	1047	74	178	379	−174	−1044	−497	−28
3.0	2359	927	−189	205	534	52	−1085	−483	192

As can be seen in Table 1, the system parameters corresponding to the higher order terms of the system dynamics (a'_{12}, a'_{22} and a'_{32} in the present example) are updated for more accuracy as larger trajectory pattern parameters (i.e. higher trajectory velocity) are employed. The smaller trajectory pattern parameters can also be seen to be enough for relatively accurate identification of the system parameters corresponding to the lower order terms of the system dynamics.

Figures 5.5 and 5.6 show that after the parameters are identified, the error on the output of the system is effectively reduced. At the same time, we may observe that the driving torque input to the system is almost all from the feed-forward signal. Therefore this system is successfully identified.

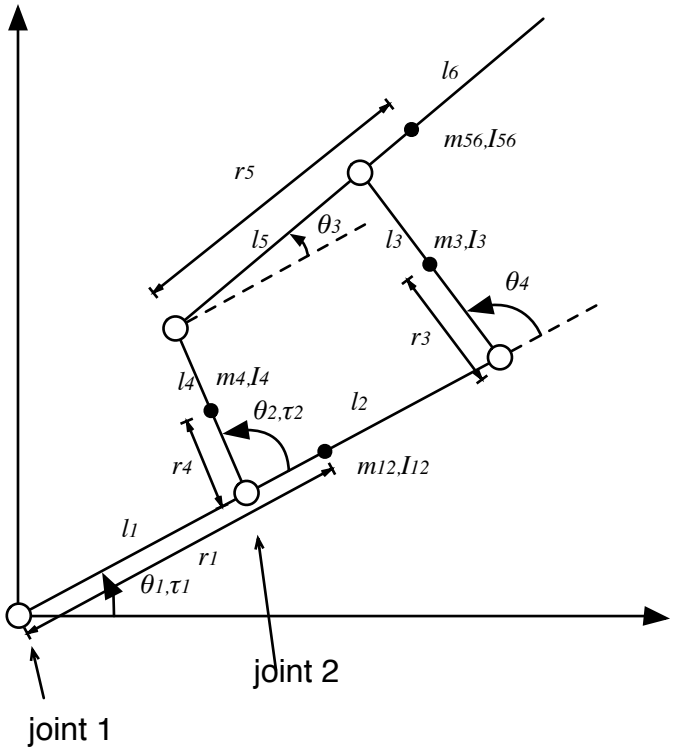

Figure 5.1: A Two Dof Closed Loop Planar Manipulator.

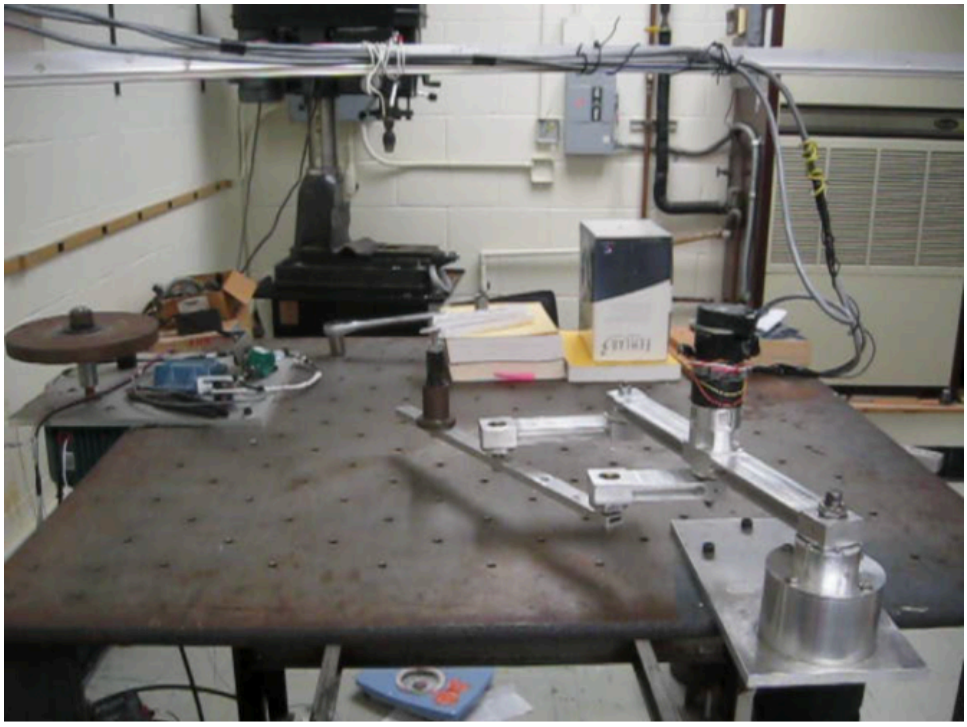

Figure 5.2: The built Two-Dof Closed Loop Planar Manipulator.

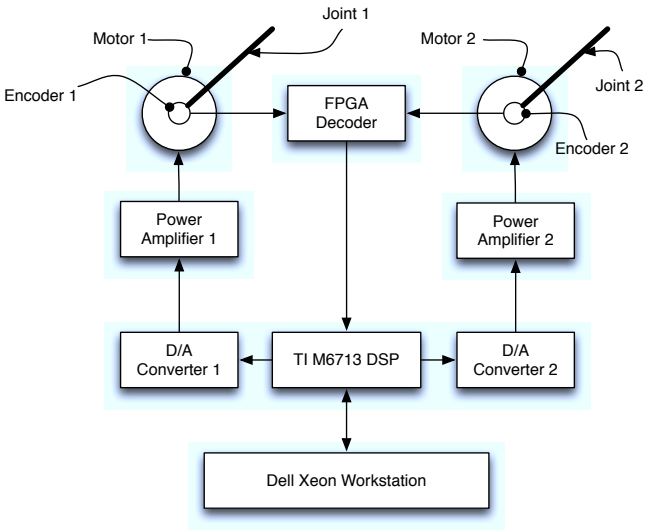

Figure 5.3: Control system schematics

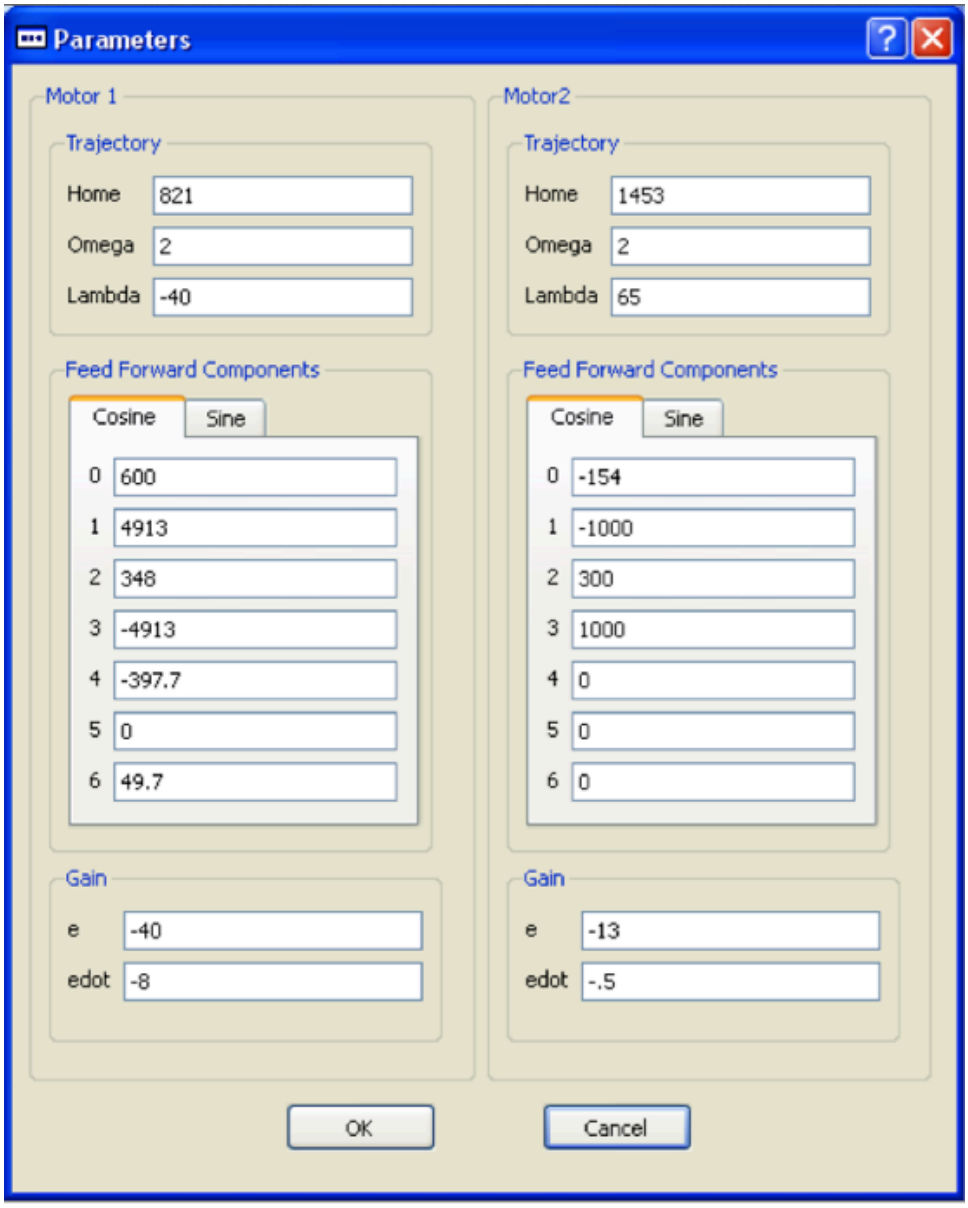

Figure 5.4: The controller program

θ_1 θ_2

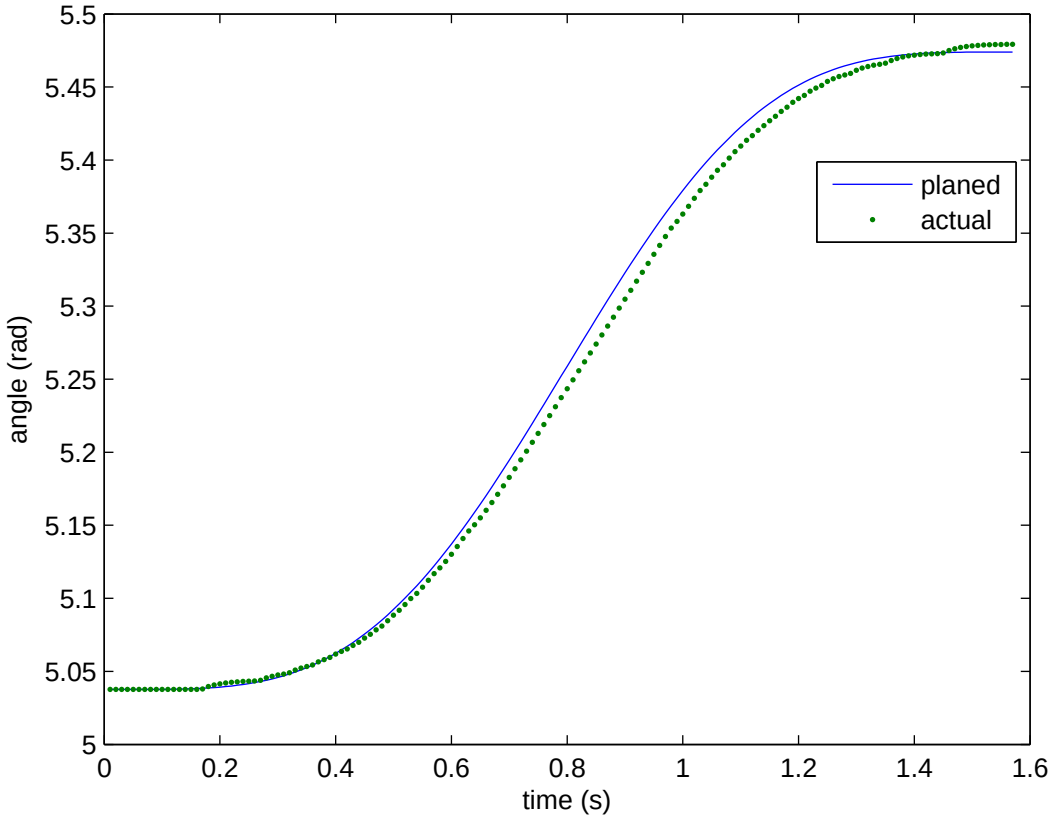

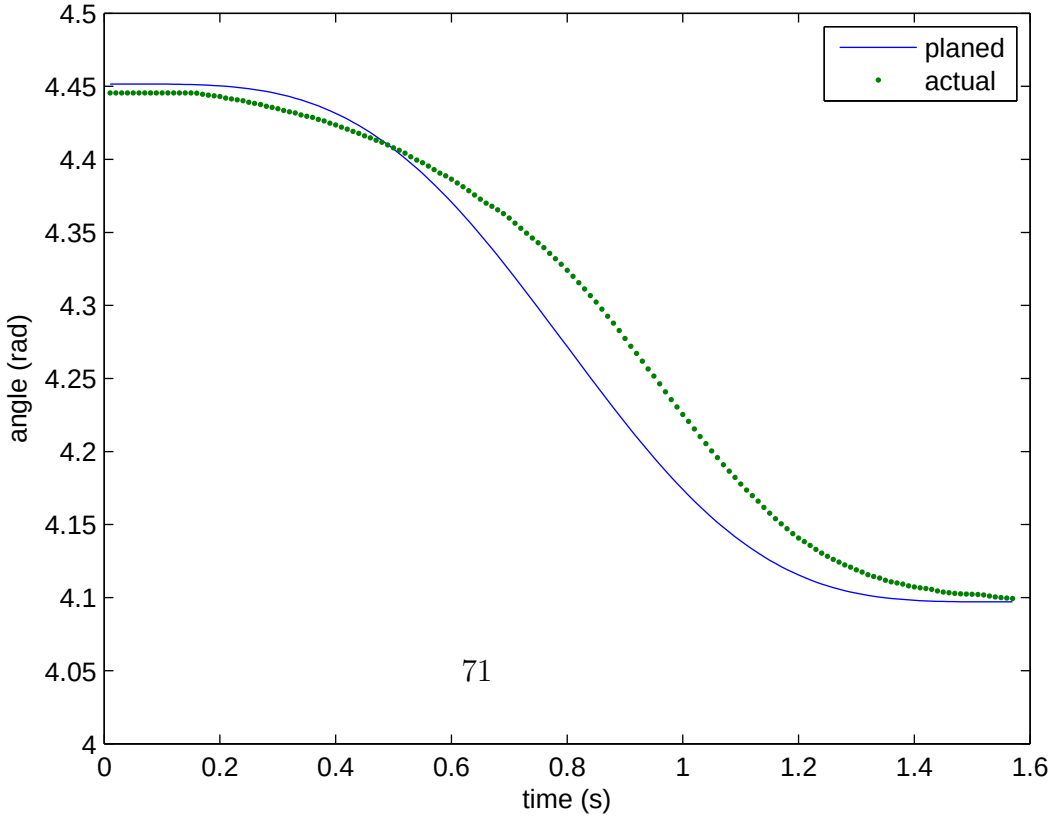

θ_1 θ_2

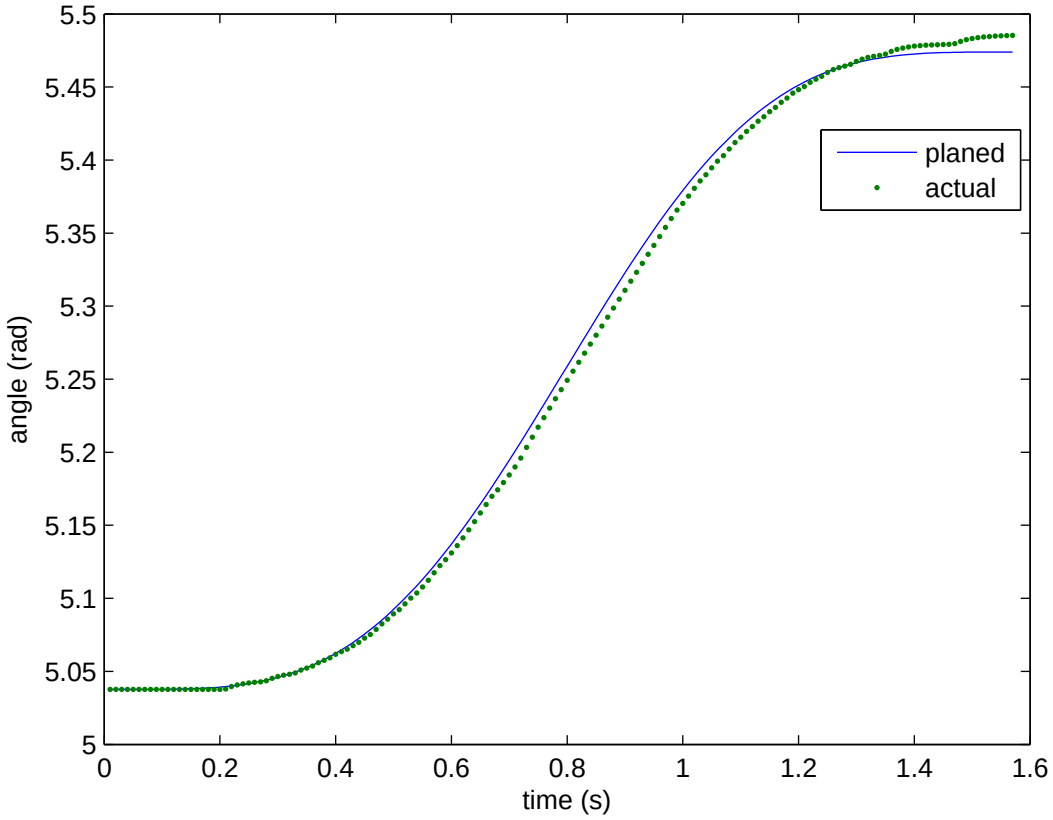

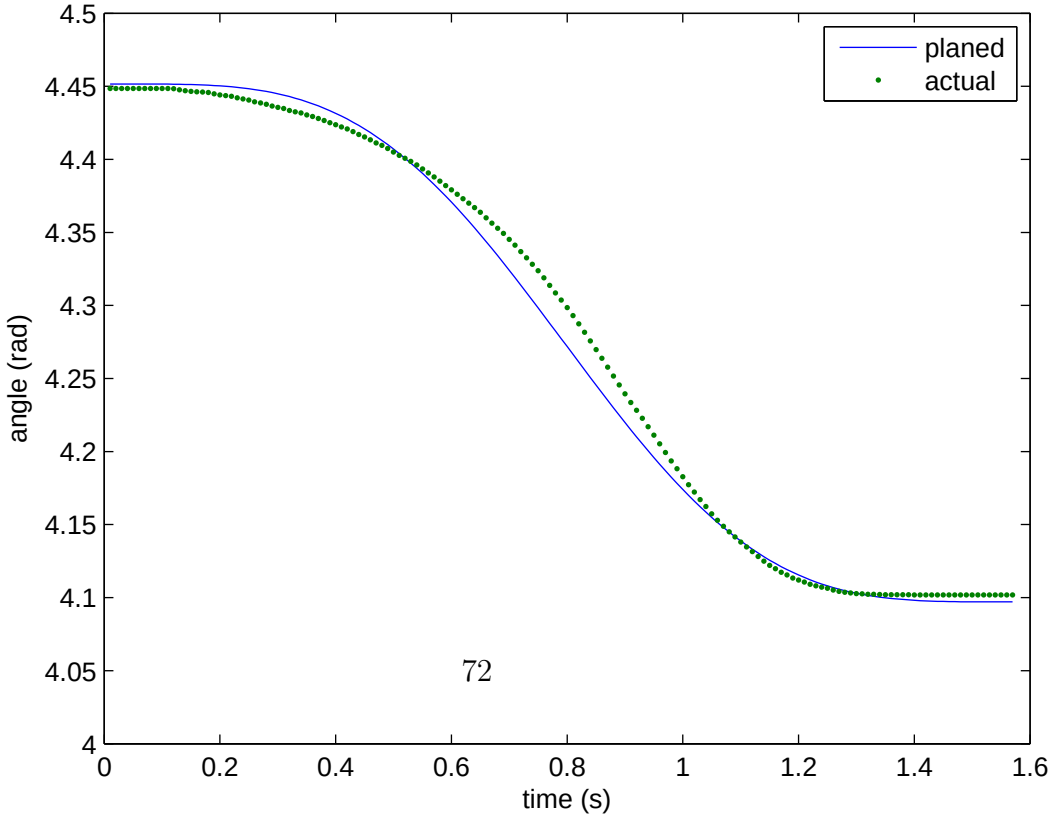

Chapter 6

On The Dynamic Response Of Actuation Devices In Nonlinear Dynamics Systems

6.1 Introduction

The dynamics of actuation devices of different types have been extensively studied. For example, a comprehensive review of studies related to different types of electrical motors is provided by Toliyat and Kliman [41]. Others have studied different methods for synthesizing trajectory and control mechanical systems with nonlinear dynamics such as robot manipulators. For example, formulation of inverse dynamics and model-based feed-forward control of dynamics systems such as robot manipulator were studied and trajectory synthesis for minimal actuation force/torque harmonics were developed using Trajectory Pattern Method (TPM) by Rastegar, et. al [13] - [33].

However, a review of published literature indicates that dynamic response issues have not been fully explained for nonlinear dynamics systems, including mechanical systems such as robot manipulators. In most current approaches to path and trajectory synthesis and control of mechanical systems, methods used for linear dynamics systems are generally employed while treating the effects of nonlinearity as input disturbances. For highly nonlinear dynamics systems, this usually means that the system operation must be relatively slow to ensure stability and effectiveness of the control system in providing operational precision. Model based feed-forward control algorithms are also used to minimize the effects of the nonlinear components of the system dynamics and to achieve better system performance in terms of operating speed and precision.

The lack of full understanding of the dynamic response characteristics and limitations of the actuation systems of mechanical systems with highly nonlinear dynamics, however, significantly reduces the effectiveness of their control system.

This chapter presents a totally new approach at studying the dynamic response requirements of mechanical systems with open-loop kinematic chain and nonlinear dynamics such as robot manipulators. It is shown that the dynamic response requirements of the system actuators can be associated with two different groups of components. The first group is shown to correspond to the components of each actuator force/torque that is "*actuator motion independent*". The dynamic response of this group of components of the actuating forces/torques is shown to be limited only by the dynamic response limitations - for the case of electrically driven actuation systems - of the driving

power amplifiers, electronics, computational and signal processing devices and components. The second group corresponds to the components of each actuator force/torque that is "*actuator motion dependent*". The dynamic response of this group of components of the actuator forces/torques is limited mainly by the effective inertia that is experienced by the actuator and its operating speed. Due to the nature of the currently available electrical, hydraulic and other actuation systems, the dynamic response of actuation systems is shown to be generally high to the former group of components and significantly lower to the latter group of components.

In this chapter, the justification for dividing the actuation forces/torques into the aforementioned two groups of components and methods for their derivation for mechanical systems with serial rigid links are presented. The reasons for dividing the actuation forces/torques into these two groups for understanding the dynamic response characteristics and limitations of mechanical systems with nonlinear dynamics are presented. The study also shows the need for the development of a new approach for feed-forward control of mechanical systems such as robot manipulators for achieving significantly higher performance in terms of speed and precision. Examples are also presented together with the discussion of the related topics of interest and future work

6.2 Actuator Motion-Dependent and Motion-Independent Components

In this section, the concept of "*motion-dependent components*" and "*motion-independent components*" of an actuator force/torque of a mechanical system is described using an example. Consider the two degrees-of-freedom planar inverse pendulum system shown in Figure 6.1. The rigid cart has a mass M and is acted on by a linear actuator providing the force F. The link (pendulum) element is considered to be massless and connected to the cart with a revolute joint, have a length L with an end mass m that can be assumed to be concentrated at the link end as shown in Figure 6.1. The pendulum link is considered to be actuated by a rotary motor that applies a torque τ to the link at the revolute joint. The displacement of the cart relative to the ground and the rotation of the link pendulum relative to the cart are indicated as x and θ, respectively.

The free body diagram of the inverse pendulum system of Figure 6.1 is shown in Figure 6.2, where F_1 and τ_1 are ground reaction force and torque and R_x and R_y are the reaction forces at the pendulum revolute joint. For the sake of simplicity, the revolute joint is considered to be located at the center of mass of the cart, where the actuation force F also acts.

Now consider the case in which the cart is held stationary and that the pendulum is undergoing a simple harmonic motion with an amplitude a given by

$$\theta = a \cos \omega t \tag{6.1}$$

From the free body diagram of Figure 6.2, the required actuation force F acting on the cart and the actuating torque τ acting on the pendulum at the revolute joint are readily seen to be

$$\begin{aligned} F &= mL(\ddot{\theta}\cos\theta - \dot{\theta}^2\sin\theta) \\ &= 4amL\omega^2\left[\cos\omega t\cos(a\cos\omega t) + a\sin^2\omega t\sin(a\cos\omega t)\right] \\ &= c_1\cos\omega t + c_2\cos 3\omega t + c_3\cos 5\omega t + ... \qquad (6.2) \\ \tau &= mL^2\ddot{\theta} = -amL\omega^2\cos\omega t \qquad (6.3) \end{aligned}$$

As can be seen in Eqn. (6.2), the actuating force F is a nonlinear function of the rotary joint motion θ (and any externally applied force, if any) and for the simple harmonic motion Eqn. (6.1), it must generally provide an actuation force that could contains several harmonics of the fundamental harmonic of the motion Eqn. (6.1) with significant amplitude. It is also noted that the force F is provided by the linear actuator driving the cart while the cart is stationary. Which means that the force F is generated by the motor power electronics by properly varying its electromagnetic forces as described in the Appendix A. In the present case, the force F described by Eqn. (6.2) is in fact a reaction force required to keep the cart stationary as the pendulum link undergoes the simple harmonic motion Eqn. (6.1). In this chapter, such components of an actuation force/torque are referred to as the "*motion independent component*" of the actuating force/torque.

In general, the dynamic response of a properly designed power electronics system driving a DC motor or the like is significantly higher than the dynamic response of the mechanical system. The dynamic response of actuation devices

are relatively high to the required "*motion independent components*" of the actuating forces/torques. As a result, the cart actuator can be expected to provide the higher harmonics of the required force, Eqn. (6.2), even for a relatively large amplitude or high fundamental frequency motions Eqn. (6.1).

On the other hand, as can be seen in Eqn. (6.3), the actuating torque is a function of its related joint motion - acceleration in this case. In this case, the actuating torque τ is required to accelerate the pendulum link with the moment of inertia mL^2 about its axis of rotation, which then cause the link to undergo its prescribed harmonic motion Eqn. (6.1) with its associated varying joint velocity. As it is shown in the Appendix A, the dynamic response of an actuator that has to accelerate a load (an effective inertia) and maintain certain constant or varying joint velocity is limited by the amount of effective load (effective inertia) and the joint velocity, both of which components may be varying. In this chapter, these components of an actuation force/torque are referred to as the "*motion dependent component*" of the actuating force/torque.

It is noted that for the sake of simplicity, in the above discussion of dynamic response limitations of the actuation devices the current and voltage limitations of the power electronics and related components - for the case of electrically driven actuation devices - are not considered. That is, the system is considered to be operating within such limitations. Such an assumption does not alter the present actuation force component division into "*motion dependent*" and "*motion independent*" components. The effects of such limitations are, however, discussed in the Appendix A.

Now for the case of the cart undergoing a simple harmonic motion $x = b\cos\omega t$ while the pendulum link is held stationary relative to the cart at an

angle $\theta = 0$, Figure 6.1, the aforementioned required actuating force and torque are readily seen to be

$$F = (M+m)\ddot{x} = -(M+m)b\omega^2 \cos\omega t \tag{6.4}$$

$$\tau = mL\ddot{x} = -mLb\omega^2 \cos\omega t \tag{6.5}$$

It is then readily observed that the required actuating torque τ is a reaction torque that is needed to keep the pendulum link at the angle $\theta = 0$, and consists only of a "*motion independent component*", Eqn. (6.5), and the dynamic response of its motor for providing the required torque is relatively high and dependent only on the dynamic response of its power electronics and related components.

The actuating force F on the other hand consists only of a "*motion dependent component*", Eqn. (6.4), and its dynamic response is relatively low and dependent on the amount of load (inertia $M + m$) and its varying velocity as indicated in the Appendix A.

Now if neither cart nor the pendulum link, Figure 6.1, are stationary, the system equations of motion become

$$\begin{aligned} F &= M\ddot{x} + mL(\ddot{\theta}\cos\theta - \dot{\theta}^2\sin\theta) + m\ddot{x} \\ &= mL(\ddot{\theta}\cos\theta - \dot{\theta}^2\sin\theta) + (M+m)\ddot{x} = F_{MI} + F_{MD} \end{aligned} \tag{6.6}$$

$$\tau = mL\ddot{x}\cos\theta + mL^2\ddot{\theta} = \tau_{MI} + \tau_{MD} \tag{6.7}$$

where $F_{MI} = mL(\ddot{\theta}\cos\theta - \dot{\theta}^2\sin\theta)$ is the "*motion independent component*" and $F_{MD} = (M+m)\ddot{x}$ is the "*motion dependent component*" of the actuating force

F acting on the cart. Similarly, $\tau_{MI} = mL\ddot{x}\cos\theta$ is the "*motion independent component*" and $\tau_{MD} = mL^2\ddot{\theta}$ is the "*motion dependent component*" of the actuating torque acting on the pendulum link.

The above separation of the actuating forces/torques into the two groups of "*motion independent components*" and "*motion dependent components*" provides the means of determining the dynamic response characteristics of such mechanical systems with highly nonlinear dynamics. As it is shown in the Appendix A, since the generation of the "*motion independent components*" of the actuating forces/torques is limited only by the dynamic response limitations of the actuator power electronics, the actuator can provide this component at relatively high frequencies demanded by the nonlinearity in the system dynamics, as for example can be seen in Eqn. (6.2) and Eqn. (6.6). However, the dynamic response of an actuator in generating the "*motion dependent components*" of the actuating forces/torques is dependent on the instantaneous actuating load (effective inertia on which it acts) and the instantaneous speed of the actuator motion.

The separation of the required actuating forces/torques into the aforementioned two groups of "*motion independent components*" and "*motion dependent components*" clearly indicates the need for a new approach to the formulation of feed-forward control signal in feed-forward control systems of mechanical systems with nonlinear dynamics that considers the dynamics response characteristics and limitations of the actuating devices such as different types of electric motors and their commonly used electronic power amplifier drivers. The general design of such feed-forward control systems and their superior performance is shown by an example in the following section.

6.3 Example And Simulation

Consider the inverse pendulum system of Figure 6.1 . The current approach for constructing a model-based feed-forward control with a linear feedback loop is shown in the block diagram of Figure 6.3. In this control system, the input desired motion x_d, θ_d and their related velocities and accelerations are used in the system equations of motion Eqn. (6.6) and Eqn. (6.7) to calculate the feed-forward force F_{ff} and torque τ_{ff}, respectively. In the block diagram of Figure 6.3, the actual position of the cart and the pendulum link are indicated as x_a and θ_a, and their velocities by $\dot{x}_a$ and $\dot{\theta}_a$, respectively. Their corresponding error signals, i.e., the difference between the desired and actual positions e_x and e_θ and desired and actual velocities $\dot{e}_x$ and $\dot{e}_\theta$, Figure 6.3, are fed back through a (usually a linear PD) controller. The sum of the feed-forward and the feedback signals is then sent to the electronic power amplifier via a low pass filter, which is used to remove the high frequency components of the signal that are considered to be beyond the dynamic response capability of the system actuators and that may excite natural modes of vibration of the system. In a system constructed as shown in Figure 6.3, the low pass filter also serves to filter other high frequency noises and disturbances. The electronic power amplifiers will then convert the filtered control signal to power signals to drive the actuating motors to produce the required actuating force and torque to drive the plant.

As was shown in the previous section, the feed-forward signal, which is generated using the system equations of motion, Eqn. (6.6) and Eqn. (6.7), contain high frequency components generated by the "*motion independent*

components" of the required actuation force/torque, which are critical for generating the desired system motion. The commonly used feed-forward control systems shown in the block diagram of Figure 6.3, however, simply filters all high frequency components of the feed-forward signal, thereby degrading the system performance in terms of speed of operation and precision.

The block diagram of the proposed model based feed-forward control system is shown in the block diagram of Figure 6.4. In this control system, the feed-forward signals corresponding to the "*motion independent components*" of the required actuating force/torque, i.e., F_{MI} and τ_{MI} in Eqn. (6.6) and Eqn. (6.7), respectively, are separated from those of "*motion dependent components*", i.e., F_{MD} and τ_{MD} in Eqn. (6.6) and Eqn. (6.7), respectively. The "*motion dependent components*" of the feed-forward signals are then similarly filtered with a low pass filter to eliminate nose and other high frequency signals that may have been generated due to the feedback signals. The "*motion independent components*" of the feed-forward signals are however either not filtered or preferably filtered with a low pass filter with significantly higher cut off frequency to eliminate higher frequency noise and components that may have been generated due to the digital nature of currently used control systems and if actual positions and velocities are not used to minimize step-like signals at each sampling time. As a result, the higher frequency components of the electronic power amplifier signals corresponding to the "*motion independent components*" of the actuating forces/torques are not eliminated by the low pass filter, thereby ensuring that the aforementioned and mainly reaction forces/torques are provided by the system actuators.

In the present example, the desired motion of the system of Figure 6.1 is

considered to be given as

$$x_d = 0.1(\cos 3t - \frac{1}{9}9t) \tag{6.8}$$

$$\theta_d = 0.6(\cos 12t - \frac{1}{9}\cos 36t) \tag{6.9}$$

The system parameters are considered to be given as $M = 10$ Kg, $m = 1$ Kg and $L = 0.4$ m. Both actuators are considered to be brushless DC motors with rotor inertia of $J = 0.35$ Kg-cm^2, and parameters $K = 0.115$ N-m/amp, $L = 7.7$ mH, $R = 4$ ohms, and $I_{max} = 12.3$ amp, Figure C.1.

The electronic power amplifier is considered to allow a maximum voltage of $V_{max} = 50$ volts and provide a peak power of $P_{peak} = 600$ watt. A gear with radius 0.02 m and a matching rack convert the rotary output from the motor to linear motion of the cart and its effective inertia is considered to be included in the mass of the cart M. The PD controller proportional and derivative gain are selected to be 1000 and 100, respectively. A second order unit gain low pass filter with undamped natural frequency $\omega_n = 100$ rad/s and the quality factor $Q = 1$ is used.

Computer simulation was performed for both control systems, Figure 6.3 and Figure 6.4 for the aforementioned desired motion. As expected, both position and velocity errors were found to be significantly smaller with the proposed feed-forward control system with the separated motion dependent and motion independent components, Figure 6.4. For example, the larger cart position error e_x for both control system simulations are shown in the plot of Figure 6.5. In this plot, the error e_x is plotted with solid line for the proposed control system, Figure 6.4, and with dashed lines for the commonly

used control system, Figure 6.3.

A close examination of the plots of the error e_x of Figure 6.5 and examination of the computer simulation results also indicates that for the commonly used feed-forward control system of Figure 6.3, the cart position error e_x is mainly due to the filtered, but required, high frequency components of the "*motion independent component*" of the actuating forces.

6.4 Conclusions

The present study clearly shows that the actuation forces/torques provided by actuation devices driving mechanical systems can be divided into two basic groups. The first group corresponding to those components of each actuator force/torque that is "actuator motion independent". The dynamic response of this group is shown to be relatively high and limited only by the dynamic response limitations - for the case of electrically driven actuation systems - of the driving power amplifiers, electronics, computational and signal processing devices and components. And the second group corresponding to those components of the actuator forces/torques that is "actuator motion dependent". The dynamic response of the latter group is shown to be relatively low and dependent on the actuator effective inertial load and actuation speed. In all mechanical systems that are properly designed, the dynamic response of the first group is significantly higher than those of the second group. By separating the required actuating forces/torques into the above two groups, the characteristics of the dynamic response of such nonlinear dynamics systems may be determined for a prescribed trajectory. The information can also be

used to significantly increase the performance of control systems of such mechanical systems by properly synthesized trajectories and control. When a feed-forward control signal is used, the performance of the system is shown to be significantly improved by generating each one of the group of components separately considering the dynamic response of the actuation system to each one of the groups of components. An example and practical methods of implementing the proposed feed-forward control for nonlinear dynamics systems are provided.

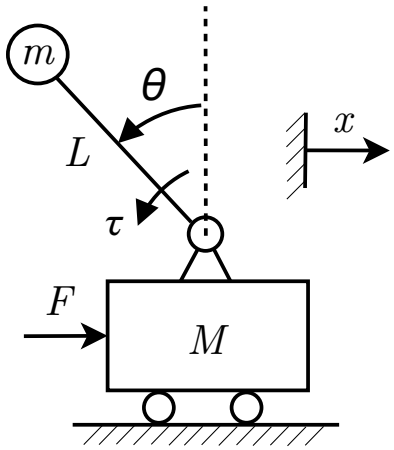

Figure 6.1: Planar inverse pendulum system.

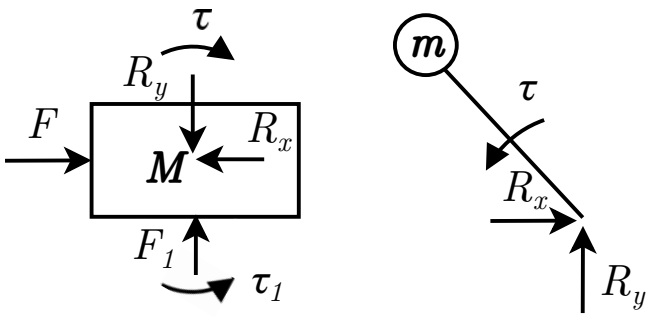

Figure 6.2: The free body diagram of the pendulum system of Figure 6.1.

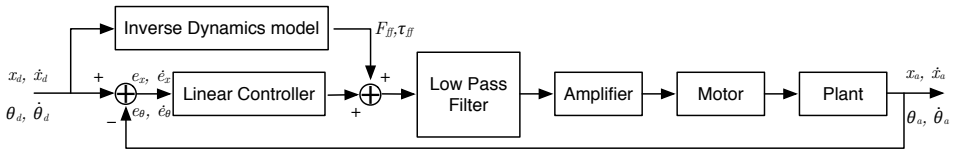

Figure 6.3: Block diagram of a commonly used feed-forward control system.

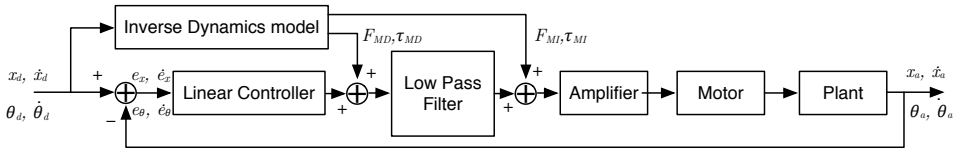

Figure 6.4: Block diagram of the proposed feed-forward control system.

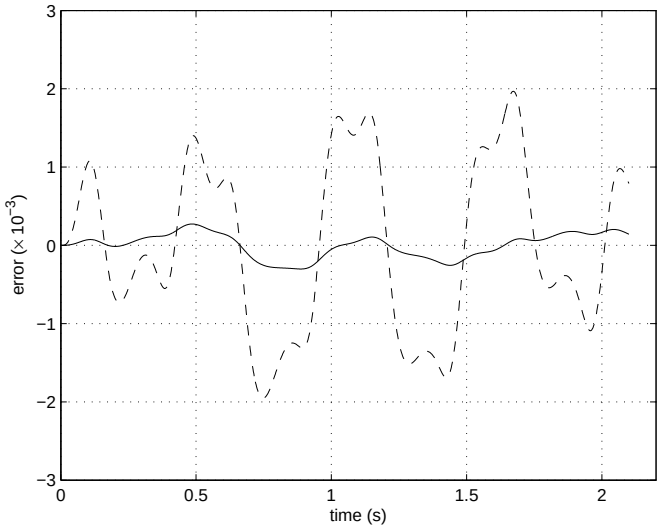

Figure 6.5: The position error for the systems of Figure 6.4 and 6.3.

Appendix A

The Differential Equations of Motion and Their Expansion

The differential equations of motion for the experiment 2-dof manipulator are

$$2f_1(\theta_2)\ddot{\theta}_1 + f_3(\theta_2)\ddot{\theta}_2 + 2\frac{df_1(\theta_2)}{d\theta_2}\dot{\theta}_1\dot{\theta}_2 + \frac{df_3(\theta_2)}{d\theta_2}\dot{\theta}_2^{\,2} = \tau_1 \qquad \text{(A.1)}$$

$$f_3(\theta_2)\ddot{\theta}_1 + 2f_2(\theta_2)\ddot{\theta}_2 - \frac{df_1(\theta_2)}{d\theta_2}\dot{\theta}_1^{\,2} + \frac{df_2(\theta_2)}{d\theta_2}\dot{\theta}_2^{\,2} = \tau_2 \qquad \text{(A.2)}$$

where

$$\begin{aligned} f_1(\theta_2) &= \frac{A_1}{2} + A_2\cos\theta_2 + A_3\cos\theta_3 + A_4\cos\theta_4 + A_5\cos(\theta_2-\theta_3) \\ f_2(\theta_2) &= \frac{A_6}{2} + \frac{A_7}{2}[\frac{l_4\sin(\theta_4-\theta_2)}{l_5\sin(\theta_3-\theta_4)}]^2 + \frac{A_8}{2}[\frac{l_4\sin(\theta_3-\theta_2)}{l_3\sin(\theta_3-\theta_4)}]^2 \\ &+ A_5\cos(\theta_2-\theta_3)\frac{l_4\sin(\theta_4-\theta_2)}{l_5\sin(\theta_3-\theta_4)} \end{aligned}$$

$$
\begin{aligned}
f_3(\theta_2) &= A_6 + A_2\cos\theta_2 + A_5\cos(\theta_2-\theta_3) \\
&+ [A_7 + A_3\cos\theta_3 + A_5\cos(\theta_2-\theta_3)]\frac{l_4\sin(\theta_4-\theta_2)}{l_5\sin(\theta_3-\theta_4)} \\
&+ (A_8 + A_4\cos\theta_4)\frac{l_4\sin(\theta_3-\theta_2)}{l_3\sin(\theta_3-\theta_4)}
\end{aligned}
$$

and where

$$
\begin{aligned}
A_1 &= m_{12}r_1^2 + I_{12} + m_3(l_1+l_2)^2 + m_3r_3^2 + I_3 \\
&+ m_4(l_1^2+r_4^2) + I_4 + m_{56}(l_1^2+l_4^2+r_5^2) + I_{56} \qquad \text{(A.3)} \\
A_2 &= m_4l_1r_4 + m_{56}l_1l_4 \qquad \text{(A.4)} \\
A_3 &= m_{56}l_1r_5 \qquad \text{(A.5)} \\
A_4 &= m_3(l_1+l_2)r_3 \qquad \text{(A.6)} \\
A_5 &= m_{56}l_4r_5 \qquad \text{(A.7)} \\
A_6 &= m_4r_4^2 + I_4 + m_{56}l_4^2 \qquad \text{(A.8)} \\
A_7 &= m_{56}r_5^2 + I_{56} \qquad \text{(A.9)} \\
A_8 &= m_3r_3^2 + I_3 \qquad \text{(A.10)}
\end{aligned}
$$

The polynomial form of the differential equations is required to reveal the harmonic pattern of error related to the parameters for identification, therefore we need to expand the functions f_1, f_2, and f_3 in a taylor series. Due to the space limitation, only the expansion of function f_1 to the first order is given as an example.

$$
f_1(\theta_2) = a_{10} + a_{11}(\theta_2-\theta_{20}) + O\left[(\theta_2-\theta_{20})^2\right] \qquad \text{(A.11)}
$$

where

$$
\begin{aligned}
a_{10} &= \frac{A_1}{2} + A_2 \cos\theta_{20} \\
&+ A_3 \cos[\arccos(\frac{{l_2}^2 - {l_3}^2 + {l_4}^2 + {l_5}^2 - 2l_2 l_4 \cos\theta_{20}}{2l_5\sqrt{{l_2}^2 + {l_4}^2 - 2l_2 l_4 \cos\theta_{20}}}) \\
&\quad -\arctan(\frac{l_4 \sin\theta_{20}}{l_2 - l_4 \cos\theta_{20}})] \\
&- A_4 \cos[\arccos(\frac{{l_2}^2 + {l_3}^2 + {l_4}^2 - {l_5}^2 - 2l_2 l_4 \cos\theta_{20}}{2l_3\sqrt{{l_2}^2 + {l_4}^2 - 2l_2 l_4 \cos\theta_{20}}}) \\
&\quad +\arctan(\frac{l_4 \sin\theta_{20}}{l_2 - l_4 \cos\theta_{20}})] \\
&+ A_5 \cos[\theta_{20} - \arccos(\frac{{l_2}^2 - {l_3}^2 + {l_4}^2 + {l_5}^2 - 2l_2 l_4 \cos\theta_{20}}{2l_5\sqrt{{l_2}^2 + {l_4}^2 - 2l_2 l_4 \cos\theta_{20}}}) \\
&\quad +\arctan(\frac{l_4 \sin\theta_{20}}{l_2 - l_4 \cos\theta_{20}})] \\
a_{11} &= -A_2 \sin\theta_{20} \\
&+ A_3(\frac{l_2 l_4({l_2}^2 + {l_3}^2 + {l_4}^2 - {l_5}^2 - 2l_2 l_4 \cos\theta_{20})\sin\theta_{20}}{2l_5({l_2}^2 + {l_4}^2 - 2l_2 l_4 \cos\theta_{20})^{3/2}\sqrt{1 - \frac{({l_2}^2 - {l_3}^2 + {l_4}^2 + {l_5}^2 - 2l_2 l_4 \cos\theta_{20})^2}{4{l_5}^2({l_2}^2 + {l_4}^2 - 2l_2 l_4 \cos\theta_{20})}}} \\
&\quad -\frac{-l_2 l_4 \cos\theta_{20} + {l_4}^2 \cos^2\theta_{20} + {l_4}^2 \sin^2\theta_{20}}{{l_2}^2 - 2l_2 l_4 \cos\theta_{20} + {l_4}^2 \cos^2\theta_{20} + {l_4}^2 \sin^2\theta_{20}}) \\
&\quad \sin[\arccos(\frac{{l_2}^2 - {l_3}^2 + {l_4}^2 + {l_5}^2 - 2l_2 l_4 \cos\theta_{20}}{2l_5\sqrt{{l_2}^2 + {l_4}^2 - 2l_2 l_4 \cos\theta_{20}}}) \\
&\quad -\arctan(\frac{l_4 \sin\theta_{20}}{l_2 - l_4 \cos\theta_{20}})] \\
&+ A_4(\frac{-l_2 l_4({l_2}^2 - {l_3}^2 + {l_4}^2 + {l_5}^2 - 2l_2 l_4 \cos\theta_{20})\sin\theta_{20}}{2l_3({l_2}^2 + {l_4}^2 - 2l_2 l_4 \cos\theta_{20})^{3/2}\sqrt{1 - \frac{({l_2}^2 + {l_3}^2 + {l_4}^2 - {l_5}^2 - 2l_2 l_4 \cos\theta_{20})^2}{4{l_3}^2({l_2}^2 + {l_4}^2 - 2l_2 l_4 \cos\theta_{20})}}} \\
&\quad -\frac{-l_2 l_4 \cos\theta_{20} + {l_4}^2 \cos^2\theta_{20} + {l_4}^2 \sin^2\theta_{20}}{{l_2}^2 - 2l_2 l_4 \cos\theta_{20} + {l_4}^2 \cos^2\theta_{20} + {l_4}^2 \sin^2\theta_{20}}) \\
&\quad \sin[\arccos(\frac{{l_2}^2 + {l_3}^2 + {l_4}^2 - {l_5}^2 - 2l_2 l_4 \cos\theta_{20}}{2l_3\sqrt{{l_2}^2 + {l_4}^2 - 2l_2 l_4 \cos\theta_{20}}})
\end{aligned}
$$

$$
\begin{aligned}
& +\arctan(\frac{l_4 \sin\theta_{20}}{l_2 - l_4 \cos\theta_{20}})] \\
+ \quad & A_5(\frac{-l_2 l_4 ({l_2}^2 + {l_3}^2 + {l_4}^2 - {l_5}^2 - 2 l_2 l_4 \cos\theta_{20}) \sin\theta_{20}}{2 l_5 ({l_2}^2 + {l_4}^2 - 2 l_2 l_4 \cos\theta_{20})^{3/2} \sqrt{1 - \frac{({l_2}^2 - {l_3}^2 + {l_4}^2 + {l_5}^2 - 2 l_2 l_4 \cos\theta_{20})^2}{4 {l_5}^2 ({l_2}^2 + {l_4}^2 - 2 l_2 l_4 \cos\theta_{20})}}} \\
& -\frac{l_2 l_4 \cos\theta_{20} - {l_4}^2 \cos^2\theta_{20} - {l_4}^2 \sin^2\theta_{20}}{{l_2}^2 - 2 l_2 l_4 \cos\theta_{20} + {l_4}^2 \cos^2\theta_{20} + {l_4}^2 \sin^2\theta_{20}} - 1) \\
& \sin[\theta_{20} - \arccos(\frac{{l_2}^2 - {l_3}^2 + {l_4}^2 + {l_5}^2 - 2 l_2 l_4 \cos\theta_{20}}{2 l_5 \sqrt{{l_2}^2 + {l_4}^2 - 2 l_2 l_4 \cos\theta_{20}}}) \\
& +\arctan(\frac{l_4 \sin\theta_{20}}{l_2 - l_4 \cos\theta_{20}})]
\end{aligned}
$$

The expansion shows that there are certain relationships between model parameters from Eqn. (A.3) through (A.10) and the approximated polynomial expansion model coefficients as a_{10} and a_{11}. During the identification, the approximated model coefficients are directly detected, and then the actual model parameters can be derived from the given relationships.

Appendix B

The Expansion to the Harmonic Form.

The expansion to the harmonic form of Eqn. (A.1) is

$$
\begin{aligned}
& 2[\Delta a_{10} + \Delta a_{11}(\theta_2 - \theta_{20}) + \Delta a_{12}(\theta_2 - \theta_{20})^2]\ddot{\theta}_1 + \\
& [\Delta a_{30} + \Delta a_{31}(\theta_2 - \theta_{20}) + \Delta a_{32}(\theta_2 - \theta_{20})^2]\ddot{\theta}_2 + \\
& 2[\Delta a_{11} + 2\Delta a_{12}(\theta_2 - \theta_{20})]\dot{\theta}_1\dot{\theta}_2 + [\Delta a_{31} + 2\Delta a_{32}(\theta_2 - \theta_{20})]\dot{\theta}_2{}^2 = \\
& -2\Delta a_{10}\lambda_1\omega^2 cos\omega t - \Delta a_{30}\lambda_2\omega^2 cos\omega t + \frac{16}{9}\Delta a_{11}\lambda_1\lambda_2\omega^2 cos\omega t \\
+ \; & \frac{8}{9}\Delta a_{31}\lambda_2{}^2\omega^2 cos\omega t - \frac{55}{27}\Delta a_{12}\lambda_1\lambda_2{}^2\omega^2 cos\omega t - \frac{55}{54}\Delta a_{32}\lambda_2{}^3\omega^2 cos\omega t \\
- \; & \frac{14}{9}\Delta a_{11}\lambda_1\lambda_2\omega^2 cos2\omega t - \frac{7}{9}\Delta a_{31}\lambda_2{}^2\omega^2 cos2\omega t \\
+ \; & \frac{224}{81}\Delta a_{12}\lambda_1\lambda_2{}^2\omega^2 cos2\omega t + \frac{112}{81}\Delta a_{32}\lambda_2{}^3\omega^2 cos2\omega t \\
+ \; & 2\Delta a_{10}\lambda_1\omega^2 cos3\omega t + \Delta a_{30}\lambda_2\omega^2 cos3\omega t - \frac{16}{9}\Delta a_{11}\lambda_1\lambda_2\omega^2 cos3\omega t
\end{aligned}
$$

$$
\begin{aligned}
- \quad & \frac{8}{9}\Delta a_{31}{\lambda_2}^2\omega^2 cos3\omega t + \frac{88}{81}\Delta a_{12}\lambda_1{\lambda_2}^2\omega^2 cos3\omega t \\
+ \quad & \frac{44}{81}\Delta a_{32}{\lambda_2}^3\omega^2 cos3\omega t + \frac{16}{9}\Delta a_{11}\lambda_1\lambda_2\omega^2 cos4\omega t \\
+ \quad & \frac{8}{9}\Delta a_{31}{\lambda_2}^2\omega^2 cos4\omega t - \frac{256}{81}\Delta a_{12}\lambda_1{\lambda_2}^2\omega^2 cos4\omega t \\
- \quad & \frac{128}{81}\Delta a_{32}{\lambda_2}^3\omega^2 cos4\omega t + \frac{100}{81}\Delta a_{12}\lambda_1{\lambda_2}^2\omega^2 cos5\omega t \\
+ \quad & \frac{50}{81}\Delta a_{32}{\lambda_2}^3\omega^2 cos5\omega t - \frac{2}{9}\Delta a_{11}\lambda_1\lambda_2\omega^2 cos6\omega t \\
- \quad & \frac{1}{9}\Delta a_{31}{\lambda_2}^2\omega^2 cos6\omega t + \frac{32}{81}\Delta a_{12}\lambda_1{\lambda_2}^2\omega^2 cos6\omega t \\
+ \quad & \frac{16}{81}\Delta a_{32}{\lambda_2}^3\omega^2 cos6\omega t
\end{aligned} \tag{B.1}
$$

The expansion to the harmonic form of Eqn. (A.2) is

$$
\begin{aligned}
& [\Delta a_{30} + \Delta a_{31}(\theta_2 - \theta_{20}) + \Delta a_{32}(\theta_2 - \theta_{20})^2]\ddot{\theta_1} + \\
& 2[\Delta a_{20} + \Delta a_{21}(\theta_2 - \theta_{20}) + \Delta a_{22}(\theta_2 - \theta_{20})^2]\ddot{\theta_2} - \\
& [\Delta a_{11} + 2\Delta a_{12}(\theta_2 - \theta_{20})]{\dot{\theta_1}}^2 + [\Delta a_{21} + 2\Delta a_{22}(\theta_2 - \theta_{20})]{\dot{\theta_2}}^2 = \\
- \quad & \frac{5}{9}\Delta a_{11}{\lambda_1}^2\omega^2 - \frac{5}{9}\Delta a_{31}\lambda_1\lambda_2\omega^2 + \frac{80}{81}\Delta a_{12}{\lambda_1}^2\lambda_2\omega^2 \\
- \quad & \frac{5}{9}\Delta a_{21}{\lambda_2}^2\omega^2 + \frac{80}{81}\Delta a_{32}\lambda_1{\lambda_2}^2\omega^2 + \frac{80}{81}\Delta a_{22}{\lambda_2}^3\omega^2 \\
- \quad & \Delta a_{30}\lambda_1\omega^2 cos\omega t - 2\Delta a_{20}\lambda_2\omega^2 cos\omega t \\
+ \quad & \frac{8}{9}\Delta a_{31}\lambda_1\lambda_2\omega^2 cos\omega t - \frac{1}{3}\Delta a_{12}{\lambda_1}^2\lambda_2\omega^2 cos\omega t \\
+ \quad & \frac{16}{9}\Delta a_{21}{\lambda_2}^2\omega^2 cos\omega t - \frac{73}{54}\Delta a_{32}\lambda_1{\lambda_2}^2\omega^2 cos\omega t
\end{aligned}
$$

$$
\begin{aligned}
- \quad & \frac{64}{27}\Delta a_{22}{\lambda_2}^3\omega^2 cos\omega t + \frac{5}{6}\Delta a_{11}{\lambda_1}^2\omega^2 cos2\omega t \\
+ \quad & \frac{1}{18}\Delta a_{31}\lambda_1\lambda_2\omega^2 cos2\omega t - \frac{40}{27}\Delta a_{12}{\lambda_1}^2\lambda_2\omega^2 cos2\omega t \\
- \quad & \frac{13}{18}\Delta a_{21}{\lambda_2}^2\omega^2 cos2\omega t - \frac{8}{81}\Delta a_{32}\lambda_1{\lambda_2}^2\omega^2 cos2\omega t \\
+ \quad & \frac{104}{81}\Delta a_{22}{\lambda_2}^3\omega^2 cos2\omega t + \Delta a_{30}\lambda_1\omega^2 cos3\omega t \\
+ \quad & 2\Delta a_{20}\lambda_2\omega^2 cos3\omega t - \frac{8}{9}\Delta a_{31}\lambda_1\lambda_2\omega^2 cos3\omega t \\
+ \quad & \frac{50}{81}\Delta a_{12}{\lambda_1}^2\lambda_2\omega^2 cos3\omega t - \frac{16}{9}\Delta a_{21}{\lambda_2}^2\omega^2 cos3\omega t \\
+ \quad & \frac{94}{81}\Delta a_{32}\lambda_1{\lambda_2}^2\omega^2 cos3\omega t + \frac{46}{27}\Delta a_{22}{\lambda_2}^3\omega^2 cos3\omega t \\
- \quad & \frac{1}{3}\Delta a_{11}{\lambda_1}^2\omega^2 cos4\omega t + \frac{5}{9}\Delta a_{31}\lambda_1\lambda_2\omega^2 cos4\omega t \\
+ \quad & \frac{16}{27}\Delta a_{12}{\lambda_1}^2\lambda_2\omega^2 cos4\omega t + \frac{13}{9}\Delta a_{21}{\lambda_2}^2\omega^2 cos4\omega t \\
- \quad & \frac{80}{81}\Delta a_{32}\lambda_1{\lambda_2}^2\omega^2 cos4\omega t - \frac{208}{81}\Delta a_{22}{\lambda_2}^3\omega^2 cos4\omega t \\
- \quad & \frac{10}{27}\Delta a_{12}{\lambda_1}^2\lambda_2\omega^2 cos5\omega t + \frac{20}{81}\Delta a_{32}\lambda_1{\lambda_2}^2\omega^2 cos5\omega t \\
+ \quad & \frac{70}{81}\Delta a_{22}{\lambda_2}^3\omega^2 cos5\omega t + \frac{1}{18}\Delta a_{11}{\lambda_1}^2\omega^2 cos6\omega t \\
- \quad & \frac{1}{18}\Delta a_{31}\lambda_1\lambda_2\omega^2 cos6\omega t - \frac{8}{81}\Delta a_{12}{\lambda_1}^2\lambda_2\omega^2 cos6\omega t \\
- \quad & \frac{1}{6}\Delta a_{21}{\lambda_2}^2\omega^2 cos6\omega t + \frac{8}{81}\Delta a_{32}\lambda_1{\lambda_2}^2\omega^2 cos6\omega t \\
+ \quad & \frac{8}{27}\Delta a_{22}{\lambda_2}^3\omega^2 cos6\omega t
\end{aligned}
\tag{B.2}
$$

Appendix C

Dynamic Response of Actuation Systems

In this section and without the loss of generality the aforementioned concept of separating the actuation forces/torques of a mechanical system into "*motion independent components*" and "*motion dependent components*" and their dynamic response limitations are presented for brushless DC motors that are driven by electronic power amplifiers.

In this section, three different actuator operation cases are studied. In the first case, the actuator is used to apply force/torque without undergoing related motion. Such forces/torques are mostly (but not entirely) reaction forces/torques, and correspond to the aforementioned "*motion independent components*" of the actuation forces/torques. In the second case, the actuator is used to apply force/torque to accelerate a load (effective inertia) and overcome back electromotive force (EMF). These actuation forces/torques correspond to the aforementioned "*motion dependent components*" of the actuation

forces/torques. In the thirds case, the actuator is used to apply a combination of "*motion independent components*" and "*motion dependent components*", a case that is generally encountered in mechanical systems with or without non-linear dynamics.

A representative model of a permanent magnet brushless rotary motor is shown in Figure C.1. In the model of Figure C.1, τ_m is an externally applied

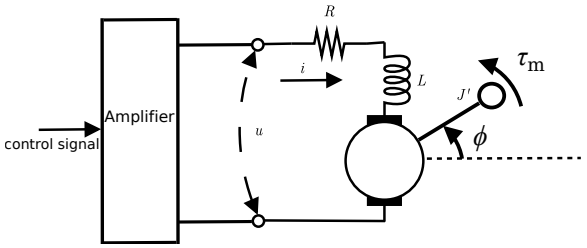

Figure C.1: Permanent magnet DC brushless electric motor model.

torque to the motor; ϕ is the motor motion (rotary for the case of present model); J' is the effective (moment of) inertia (load) experienced by the motor; i is the armature current; R and L are the resistance and inductance of armature coil, respectively; and u is the voltage across the armature coil.

The dynamics of brushless DC motor of Figure C.1 can be described by the following two coupled second order ordinary differential equations

$$\tau_m = k_t i - J'\ddot{\phi} \tag{C.1}$$

$$u = iR + L\dot{i} + k_v\dot{\phi} \tag{C.2}$$

where k_t is the motor torque constant; and k_v is the motor velocity related back EMF coefficient constant, which is determined by the flux density of the permanent magnets, the reluctance of the iron core of the armature, and the

number of turns of the armature winding.

In all electric motors, the maximum allowable armature current i and voltage u are limited. These limits are hereinafter indicated by

$$i \leq I_{max} \tag{C.3}$$

$$u \leq U_{max} \tag{C.4}$$

where I_{max} is the maximum allowable armature current (motor stall current) and U_{max} is allowable armature voltage. In a properly designed actuation system, the electronic power amplifier is designed to provide the above maximum armature current and voltage.

When used to drive a mechanical system, the actuator electronic power amplifier, Figure C.1, receives a control signal corresponding to the desired actuation force/torque from the system controller and transmits electric current to the motor armature to produce the said actuation force/torque.

As an electronic device, the electronic power amplifier dynamic response (for most mechanical system operations, the bandwidth of its linear frequency response) is significantly higher than the dynamic response of any practical mechanical system, even when its inertia load is only the very lightweight rotor of the motor. The dynamic response limitation of the actuation system operating a pure inertia load may be approximated by the "cut off" frequency presented later in this section.

Thereby considering the fact that in a properly designed actuation system such as the one shown in Figure C.1 the dynamic response of the system electronic power amplifier is significantly higher than those of any practical

mechanical system, we may safely assume that in operating a properly designed mechanical system, the dynamic response limitations of the system electronic power amplifier could even be neglected. For the system shown in Figure C.1, this assumption also means that for operating a mechanical system, no frequency limitation needs to be considered on the system electronic power amplifier for providing the required voltage u and current i. The aforementioned maximum available voltage, U_{max} and current I_{max} are obviously still applicable.

The Case of No-Motion Force/Torque Application

In this case, the motor is kept stationary, i.e., $\dot{\phi} = 0$, and is only required to provide the torque τ_m, Figure C.1, to resist the externally applied torque of the same magnitude but opposite sign. Now let the torque τ_m be represented in the form of Fourier series with j number of significant harmonics as

$$\tau_m = \sum_j a_j \cos(j\omega t + \psi_j)$$

Then from Eqn. (C.1) and Eqn. (C.2), the required armature current i and voltage across the coil u are readily seen to become

$$\begin{aligned} i &= \frac{\tau_m}{k_t} = \sum_j I_j \cos(j\omega t + \psi_j) \qquad \text{(C.5)} \\ u &= iR + L\dot{i} \\ &= R\sum_j I_j \cos(j\omega t + \psi_j) - L\sum_j I_j j\omega \sin(j\omega t + \psi_j) \\ &= \sum_j I_j \sqrt{R^2 + L^2 j^2 \omega^2} cos(j\omega t + \psi_j') \qquad \text{(C.6)} \end{aligned}$$

where $I_j = \frac{a_j}{k_t}$ and ψ_j are the amplitude and phase of the jth harmonic of the required current i.

As can be seen from Eqn. (C.5) and Eqn. (C.6), as long as the aforementioned maximum current and voltage levels I_{max} and U_{max} are not reached and as long as the electronic power amplifier can provide the highest harmonic in the torque τ_m, then the actuator can provide the above required torque τ_m.

At this point it might be of interest to note that the corresponding required power P from the electronic power amplifier for generating the above toque τ_m is

$$P = ui = i^2R + Li\dot{i} \tag{C.7}$$

Thereby making the average power requirement

$$P_{aver} = \frac{1}{T}\int_0^T Pdt = \frac{1}{T}\int_0^T i^2Rdt = \sum_j \frac{I_j^2R}{2} \tag{C.8}$$

where T is the period of the fundamental frequency ω. As expected, since the actuator does not do any work on a load (inertia), the consumed power is only due to the coil resistance R.

The Case of "Motion-Generating" Actuation Force/Torque

In this section, the actuator is considered to apply a required level of force/torque to a load (effective inertia) to achieve a desired motion (acceleration and velocity) profile. The brushless DC motor and its electronic power amplifies of Figure C.1 is still being used.

In current practice, the frequency response of motor velocity is defined in terms of the armature (with effective load) speed versus voltage and without any externally applied torque (τ_m in Figure C.1). Using a linear model of the motor, a cut off frequency [41] is then defined using the transfer function between the voltage $V(s)$ and speed $\Omega(s)$ after Laplace transform as

$$G(s) = \frac{\Omega(s)}{V(s)/K} = \frac{1}{(s^2/\omega_n^2) + 1} \tag{C.9}$$

where $K = k_v = k_t$, $\omega_n = \frac{K}{\sqrt{LJ'}}$. The natural frequency ω_n is considered to be a cut off frequency, i.e., the highest frequency that the electric motor can effectively operate.

From the discussion of the previous no-motion force application case, it is obvious that the above cut off frequency cannot be used to determine the dynamic response of general mechanical systems (even if their dynamics were not non-linear) since it only considers the motion response.

In this section we define a cut off frequency that considers the characteristics of both the electric motor as well as its electronic power amplifier. Here, a cut off frequency ω_c is still defined in the absence of any externally applied force/torque to the motor and the limiting factors considered are the aforementioned maximum current I_{max} and maximum voltage U_{max} that the electronic power amplifier can provide and that the motor armature can tolerate.

Consider the case in which the motor is undergoing the simple harmonic motion

$$\phi = \lambda_\phi \cos \omega_\phi t \tag{C.10}$$

By substituting the motion of Eqn. (C.10) into Eqn. (C.1) and setting the externally applied torque $\tau_m = 0$, and for the aforementioned maximum armature current of I_{max}, we get

$$k_t I_{max} \cos \omega_c t = J' \lambda_\phi \omega_c^2 \cos \omega_c t \tag{C.11}$$

From which our previously described cut off frequency can be seen to become

$$\omega_c = \sqrt{\frac{k_t I_{max}}{\lambda_\phi J'}} \tag{C.12}$$

As can be expected, Eqn. (C.12) indicates that higher the maximum current I_{max} and lower the motion amplitude and motor inertia load, higher will be the maximum motion or cut off frequency as previously defined.

In addition, from Eqn. (C.2), the voltage u required to achieve the motion Eqn. (C.10) at the cut off frequency ω_c becomes

$$\begin{aligned} u &= I_{max} R \cos \omega_c t - (L I_{max} + k_v \lambda_\phi) \omega_c \sin \omega_c t \\ &= \sqrt{I_{max}^2 R^2 + (L I_{max} + k_v \lambda_\phi)^2 \omega_c^2} \cos(\omega_c t + \alpha) \end{aligned} \tag{C.13}$$

where

$$\alpha = \arccos \frac{I_{max} R}{\sqrt{I_{max}^2 R^2 + (L I_{max} + k_v \lambda_\phi)^2 \omega_c^2}}$$

Eqn. (C.13) provides the corresponding level of voltage that the electronic power amplifier has to provide. However, this is not the maximum voltage that the electronic power amplifier has to provide since during the motion, the motor velocity generates back EMF, which the electronic power amplifier

must also counter. The maximum level of generated back EMF voltage is proportional to the motor velocity, which becomes higher with higher motion frequency and amplitude, Eqn. (C.10).

The Case of Combined External and Motion-Generated Actuation Force/Torque

Now consider the case in which the motor is providing the simple harmonic motion described by Eqn. (C.10) while at the same time it has to resist and externally applied torque

$$\tau_m = \lambda_m \cos \omega_m t \tag{C.14}$$

Substituting Eqn. (C.14) and Eqn. (C.10) into Eqn. (C.1) and solving for the current i, we obtain

$$i = \frac{1}{k_t}(-J'\lambda_\phi \omega_\phi^2 \cos \omega_\phi t + \lambda_m \cos \omega_m t) \tag{C.15}$$

Eqn. (C.15) clearly shows that required i can be separated into two distinct components. The first (left) component being motion related, and its magnitude increases with the load (effective inertia), amplitude of the simple harmonic motion and square of the motion frequency. This component of the required current corresponds to the aforementioned "*motion dependent component*" of the actuating torque. The ability of the motor to provide this component of the torque is limited by the aforementioned cut off frequency ω_c, and the system maximum current I_{max} and maximum voltage U_{max} that

either the electronic power amplifier can provide or that the motor armature can withstand.

The second component is not motion related and is due to the reaction that the motor has to provide to resist the externally applied torques. This component corresponds to the aforementioned "*motion independent component*" of the actuating torque. And the ability of the motor to provide this component of the torque is only limited by the system maximum current I_{max} and maximum voltage U_{max}, and the dynamic (frequency) response of the electronic power amplifier, which if it is properly designed, is orders of magnitude higher than the motor cut off frequency ω_c.

The corresponding required voltage u can then be obtained from Eqn. (C.2) to be

$$\begin{aligned} u &= \frac{R}{k_t}(\lambda_m \cos\omega_m t - J'\lambda_\phi \omega_\phi^2 \cos\omega_\phi t) - \\ &\quad \frac{L}{k_t}(\lambda_m \omega_m \sin\omega_m t - J'\lambda_\phi \omega_\phi^3 \sin\omega_\phi t) - k_v \lambda_\phi \omega_\phi \sin\omega_\phi t \\ &= \frac{\lambda_\phi \omega_\phi}{k_t}\sqrt{J'^2\omega_\phi^2 R^2 + \left(J'\omega_\phi^2 L + k_t k_v\right)^2}\cos(\omega_\phi t + \alpha_\phi) + \\ &\quad \frac{\lambda_m}{k_t}\sqrt{R^2 + L^2\omega_m^2}\cos(\omega_m t + \alpha_m) \end{aligned} \tag{C.16}$$

where α_m and α_ϕ are the phases. The Eqn. (C.16) clearly shows that similar to the required current, Eqn. (C.15), the required voltage u also has the aforementioned two distinct components.

The first (left) component being motion related, and its magnitude increases with the load (effective inertia), amplitude of the simple harmonic motion and its frequency. This component of the required current corresponds to

the aforementioned "*motion dependent component*" of the actuating torque. The ability of the motor to provide this component of the torque is limited by the aforementioned cut off frequency ω_c, and the system maximum current I_{max} and maximum voltage U_{max} that either the electronic power amplifier can provide or that the motor armature can withstand.

The second component is not motion related and is due to the reaction that the motor has to provide to resist externally applied torques. This component corresponds to the aforementioned "*motion independent component*" of the actuating torque. And the ability of the motor to provide this component of the torque is only limited by the system maximum current I_{max} and maximum voltage U_{max}, and the dynamic (frequency) response of the electronic power amplifier, which if it is properly designed, is orders of magnitude higher than the motor cut off frequency ω_c.

Bibliography

[1] Lin, C.S., Chang, P.R.,Luh, J.Y.S., "Formulation and Optimization of Cubic Polynomial Joint Trajectories for Industrial Robots.", *IEEE Trans. Auto. Control, AC-28*, 1983,(12), p 1066-1073

[2] Fu, K S., Gonzalez,R.C., Lee, C.S.G., "ROBOTICS: Control, Sensing, Vision, and Intelligence", *McGraw-Hill*, 1987, 580pp.

[3] Johnson, E.R., Murphey, T.D., "Automated Trajectory Synthesis from Animation Data Using Trajectory Optimization", *Automation Science and Engineering, 2009. CASE 2009. IEEE International Conference on (978-1-4244-4578-3)*,22-25 Aug. 2009. p.274

[4] Korayem, M.H., Nikoobin, A., Azimirad, V., "Trajectory optimization of flexible link manipulators in point-to-point motion" *Robotica*, 2009, v 27, p 825-840

[5] Rastegar, J., "A 'basis trajectory' approach to the inverse dynamics formulation of robot manipulators", *Proc 90 Int Conf Syst Eng*, 1990, p 308-311

[6] Fardanesh, B., Rastegar, J., "A new model based tracking controller for robot manipulators using the trajectory pattern inverse dynamics", *Proceedings - IEEE International Conference on Robotics and Automation*, v 3, 1992, p 2152-2157

[7] Rastegar, J.,Tu, Q., Mattice, M., Coleman, N. Source, "Trajectory pattern method applied to a nonlinear flexible pointing system", *American Control Conference*, 1993, p 1622-1626

[8] Tu, Q., Rastegar, J., Singh, R.J., "Trajectory Synthesis and Inverse Dynamics Model Formulation and Control of tip Motion of a High Performance Flexible Positioning System", *Mechanism and Machine Theory*, 1994, 29(7), p 959-968

[9] Tu, Q., Rastegar, J., "Manipulator Trajectory Synthesis for Minimal Vibrational Excitation Due to Payload" *Trans. of the Canadian Society of Mechanical Engineers*, 1993, 17(4A), p 557-566

[10] Ge, Q.J.; Rastegar, J., "Low-harmonic rational Bezier and spline curves for joint trajectory synthesis with actuator dynamics response limitations", *Robotics and Automation, 1995. Proceedings., 1995 IEEE International Conference on (0-7803-1965-6)*, 1995, v 3, p 2433

[11] Ge, Q.J.; Rastegar, J., "Bernstein-Bezier Harmonics and Their Application to Robot Trajectory Synthesis With Minimal Vibrational Excitation", *JOURNAL OF MECHANICAL DESIGN*, DEC 1996, V 118, Iss 4 ,p 509-514

[12] Rastegar, J., Feng, D., "Proceeding: Model Parameter Estimation of Nonlinear Systems by Trajectory Pattern Method", ACME Conference, 2010

[13] Rastegar, J., and Liu, L., 1999, "Task Specific Optimal Simultaneous Kinematic, Dynamic and Control Design of High Performance Manipulators", *ASME/IEEE Trans. on Mechatronics*, **4** (4), pp. 387-395.

[14] Ibarra, R. and Perreira, N.D., 1986, "Determination of Linkage Parameter and Pair Variable Errors in Open Chain Kinematic Linkages Using a Minimum Set of Pose Measurement Data", *ASME J. Mech., Tran. and Aut. in Des.*, **108**, pp. 159-166.

[15] Kazerounian, K. and Qian, G.Z., 1988, "Kinematic Calibration of Robotic Manipulators", *ASME J. Mech., Tran. and Aut. in Des.*, **111**, pp. 482-487.

[16] Goswami, A. and Bosnik, J.R., 1993, "On the Relationship Between the Physical Features of Robotic Manipulators and the Kinematic Parameters Produced by Numerical Calibration", *ASME J. Mech., Tran. and Aut. in Des.*, **115**, pp. 892-900.

[17] Kaizerman, S., Zak, G., Benhabib, B. and Fenton, R.G., 1994, "A Sensitivity Analysis Based Method for Robot Calibration", *ASME J. Mech., Tran. and Aut. in Des.*, **116**, pp. 607-613.

[18] Zak, G., Benhabib, B., Fenton, R.G. and Saban, C., 1994, "Application of the Weighted Least Squares Parameter Estimation Method to the Robot Calibration", *ASME J. Mech., Tran. and Aut. in Des.*, **116**, pp. 890-893.

[19] Guo, L. and Angeles, J., 1989, "Controller Estimation for the Adaptive Control of Robotic Manipulator", *J. of Robo. and Aut.*, **5**, pp. 315-323.

[20] Kawasaki, H. and Nishimura, K., 1988, "Terminal Link Parameter Estimation of Robotic Manipulator", *J. of Robo. and Aut.*, **4**, pp. 485-490.

[21] Swevers, J., Ganseman, C., Schulter, J.D. and Brusset, H.V., 1997, "Optimal Robot Excitation and Identification", *J. of Robo. and Aut.*, **13**, pp. 730-740.

[22] Lin, S.K., 1992, "An Identification Method for Estimating the Inertia Parameters of a Manipulator", *J. of Rob. Sys.*, **9**, pp. 505-528.

[23] Lin, S.K., 1994, "An Approach to the Identifiable Parameters of a Manipulator", *J. of Rob. Sys.*, **11**, pp. 641-656.

[24] Dolanc, G., Strmcnik, S., 2005, "Identification of nonlinear systems using a piecewise linear Hammerstein model", *Sys. and Cont. Letters*, **54**, pp. 145-158.

[25] Kenne, G., Ahmed-Ali, A., Lamnabhi-Lagarrigue, F., Nkwawo, H., 2006, "Nonlinear system parameters estimation using radial basis function network", *Control Eng. Practice*, **14**, pp. 819-832.

[26] Spottswood, S.M., and Allemang, R. J., 2006, "Identification of nonlinear parameters for reduced order models", *J. of Sou. and Vib.*, **295**, pp. 226-245.

[27] Li, K., Peng, J.X., Bai, E.W., 2006, "A two-stage algorithm for identification of nonlinear dynamic systems", *Automatica*, **42**, pp. 1189-1197.

[28] Gray, G.J., Murray-Smith, D.J., Li, Y., Sharman, K.C., Weinbrenner, T., 1998, " Nonlinear model structure identification using genetic programming", *Control Eng. Practice*, **6**, pp. 1341-1352.

[29] Abdelazim, T., and Malik, O.P., 2005, "Identification of nonlinear systems by Takagi-Sugeno fuzzy logic grey box modeling for real time control", *Control Eng. Practice*, **13**, pp. 1489-1498.

[30] Chen, S., Billings, S.A., and Luo, W., 1989, "Orthogonal least squares methods and their application to nonlinear system identification", *Inter. J. of Control*, **50**(5), pp.1873-1896.

[31] Poroddi, L., and Spinelli, W., 2003, "An identification algorithm for polynomial narx models based on simulation error minimization", *Inter. J. of Control*, **76**, pp.1767-1781.

[32] Zhu, Q.M., and Billings, S.A., 1996, "Fast orthogonal identification of nonlinear stochastic models and radial basis function neural networks", *Inter. J. of Control*, **64** (5), pp.871-886.

[33] Rastegar, J., and Fardanesh, B., 1990, "Trajectory Pattern Specific Inverse Dynamics Formulation of Robot Manipulators and its Applications", *1990 ASME Mech. Conf.*.

[34] Rastegar, J., and Fardanesh, B., 1990, "A Basis Trajectory Approach to the Inverse Dynamics Formulation of Robot Manipulators", *IEEE Int. Conf. on Sys. Eng.*

[35] Fardanesh, B., and Rastegar, J., 1990, "Model Based Controllers for Robot Manipulators Using Basis Trajectory Inverse Dynamics", *IEEE Int. Conf. on Sys. Eng.*

[36] Rastegar, J. and Fardanesh, B., 1991, "Inverse Dynamics Models of Robot Manipulators Using Trajectory Patterns - With Application to Learning Controllers", *Eighth World Cong. on the Theory of Machines and Mechanisms.*

[37] Fardanesh, B., and Rastegar, J., 1992, "A New Model Based Tracking Controller for Robot Manipulators Using The Trajectory Pattern Inverse Dynamics", *IEEE Trans. Rob. and Auto.*, **8** (2), pp. 279-285.

[38] Rastegar, J., Tu, Q., Fardanesh, B., Coleman, N. and Mattice, M., 1992, "Experimental Implementation of Trajectory Pattern Inverse Dynamics Model Based Controller for a Flexible Structure", *1992 American Control Conf.*

[39] Rastegar, J., Tu, Q., Mattice, M. and Coleman, N., 1993, "Trajectory Pattern Method applied to a Nonlinear Flexible Pointing System", *1993 American Control Conf.*

[40] Tu, Q. and Rastegar, J., 1999, "On the Inherent Characteristics of the Dynamics of Robot Manipulators", *Mechanisms and Machine Theory*, **34**, pp. 171-191.

[41] Toliyat, H. A., Kliman, G. B., 2004, *HANDBOOK OF ELECTRIC MOTORS*, 2nd ed., Taylor and Francis Group, 6000 Broken Sound Parkway NW, Suite 300 Boca Raton, FL 33487-2742.